

Article

Enhanced Cd Tolerance in Bamboo: Synergistic Effects of Nano-Hydroxyapatite and Fe₃O₄ Nanoparticles on Reactive Oxygen Species Scavenging, Cd Detoxification, and Water Balance

Abolghassem Emamverdian ^{1,2,*} , Ahlam Khalofah ^{3,4} , Necla Pehlivan ⁵  and Yang Li ⁶

¹ Co-Innovation Center for Sustainable Forestry in Southern China, Nanjing Forestry University, Nanjing 210037, China

² Bamboo Research Institute, Nanjing Forestry University, Nanjing 210037, China

³ Biology Department, Faculty of Science, King Khalid University, P.O. Box 9004, Abha 61413, Saudi Arabia; aalshayeed@kku.edu.sa

⁴ Research Center for Advanced Materials Science (RCAMS), King Khalid University, P.O. Box 9004, Abha 61413, Saudi Arabia

⁵ Department of Biology, Recep Tayyip Erdogan University, Rize 53100, Türkiye; necla.pehlivan@erdogan.edu.tr

⁶ Department of Mathematics and Statistics, Florida Atlantic University, Boca Raton, FL 33431, USA; yangli@fau.edu

* Correspondence: emamverdiyan@njfu.edu.cn; Tel.: +86-15850741241

Abstract: Nano-hydroxyapatite (n-HAP) and Fe₃O₄ NPs (Fe₃O₄ NPs) offer effective and economical approaches for reducing Cd toxicity, which presents considerable risks to both environmental and human health. We examined the mechanisms through which these NPs mitigate Cd toxicity in bamboo, *Pleioblastus pygmaeus*. The plants were exposed to Cd (0, 50, 100, and 150 mg L⁻¹) and received foliar sprays of 100 mg L⁻¹ n-HAP, 100 mg L⁻¹ Fe₃O₄ NPs, and a combination of both treatments. The findings indicated that Cd exposure led to oxidized molecules in bamboo, as evidenced by elevated levels of reactive oxygen species (ROS) and lipoperoxidation. Foliar treatments utilizing n-HAP and Fe₃O₄ NPs markedly diminished these effects. H₂O₂, O₂•⁻, malondialdehyde (MDA), and electrolyte leakage (EL) levels decreased by 56%, 71%, 65%, and 72%, respectively, compared to the controls. The application of n-HAP and Fe₃O₄ NPs significantly enhanced the enzymes, including superoxide dismutase (SOD), peroxidase (POD), catalase (CAT), glutathione reductase (GR), and phenylalanine ammonia-lyase (PAL), with increases observed between 28% and 56%. Furthermore, there was an enhancement in proline accumulation, total phenolic content (TPC), flavonoids (TFC), nitric oxide levels, relative water content (RWC), chlorophyll concentration, and photosynthetic parameters. The combination of n-HAP and Fe₃O₄ NPs was most effective in improving bamboo tolerance to Cd, especially at moderate Cd concentrations of 50 and 80 mg L⁻¹. The results indicate that n-HAP and Fe₃O₄ NPs, particularly in combination, may mitigate Cd toxicity by decreasing Cd uptake, improving antioxidant capacity, and preserving plant water balance.

Keywords: bamboo; Cd; Fe₃O₄ NPs; n-HAP; stress; tolerance



Academic Editor: Daniela Romano

Received: 6 January 2025

Revised: 28 January 2025

Accepted: 30 January 2025

Published: 31 January 2025

Citation: Emamverdian, A.; Khalofah, A.; Pehlivan, N.; Li, Y. Enhanced Cd Tolerance in Bamboo: Synergistic Effects of Nano-Hydroxyapatite and Fe₃O₄ Nanoparticles on Reactive Oxygen Species Scavenging, Cd Detoxification, and Water Balance. *Agronomy* **2025**, *15*, 386. <https://doi.org/10.3390/agronomy15020386>

Copyright: © 2025 by the authors. Licensee MDPI, Basel, Switzerland. This article is an open access article distributed under the terms and conditions of the Creative Commons Attribution (CC BY) license (<https://creativecommons.org/licenses/by/4.0/>).

1. Introduction

In recent decades, increased anthropogenic activity has significantly contributed to environmental pollution, particularly heavy metal contamination, which poses a direct and indirect threat to human life [1,2]. Several studies have highlighted the role of heavy

metals as a major environmental hazard, impacting not only the environment but also animals, agricultural land, and plants, ultimately threatening the food chain [3–5]. It has been reported that a wide range of China's farmland (19.4%) and forestland (10.0%), especially bamboo forestland soil, is contaminated by heavy metals [6]. Cadmium has the highest percentage of toxicity (7%) in Chinese agricultural soil as well as urban areas [7–9]. Cadmium (Cd) is considered one of the most prevalent and harmful heavy metals, with no positive impact on plant growth [10]. As a non-essential element, Cd, when absorbed by plants, generates reactive oxygen species (ROS), causing free radical stress within plant cells [11,12]. This oxidative stress can disrupt cellular functions, damaging proteins, lipids, and nucleic acids, and result in membrane lipid peroxidation [12]. Furthermore, Cd negatively affects the plant defense system, impeding antioxidant capacity and leading to reduced photosynthetic efficiency, stunted growth, and eventual plant death [12].

In recent years, nanotechnology has opened new avenues in various fields, including agriculture and environmental remediation [13]. Among the most promising nanoparticles (NPs) for these applications are nano-hydroxyapatite (n-HAP) and iron oxide (Fe_3O_4) nanoparticles. Fe_3O_4 NPs are particularly useful due to their non-toxic nature and easy synthesis, making them effective adsorbents for wastewater treatment [14,15]. These NPs have also been shown to enhance nutrient uptake and trigger growth [16,17]. The use of Fe_3O_4 NPs in mitigating Cd toxicity has been explored in seed priming [18], in the accumulation of Cd in wheat [19], and in the reduction in lead content in *Basella alba* L. [18]. On the other hand, n-HAP is a safe material with a strong affinity for organic compounds, making it an effective tool for environmental remediation. With its small particle size and large surface area, n-HAP can interact strongly with metal ions, which enhances its ability to stabilize heavy metals like Cd and Pb in the soil [20–22]. Many studies have shown that n-HAP can improve soil quality and serve as a nano-fertilizer, promoting crop production in areas with heavy metal toxicity [23,24]. Furthermore, n-HAP and Fe_3O_4 NPs are known to regulate heavy metal uptake in plants, with studies demonstrating their effectiveness in reducing Cd accumulation in *Amaranthus tricolor* L. and Pb accumulation in ryegrass [25,26]. It has been reported that n-HAP has the ability to immobilize cadmium through ion exchange and surface complexation [27]. In another study, Fe_3O_4 NPs increase plant tolerance to arsenic stress by modulating antioxidant enzyme activities [28]. However, these studies occur in controlled environments, and their applicability in field conditions still needs more investigation. A reduction in heavy metals by the combination of n-HAP nanoparticles and Fe_3O_4 NPs to immobilize Pb and Cd in contaminated soils was reported by Wu et al. (2023), who demonstrated that the combination form of these two nanoparticles improved efficiency compared to individual nanoparticles [29]. Although the potential benefits of these NPs are clear, there are concerns regarding their phytotoxicity and the potential for causing oxidation in cells due to their high reactivity/large surface area [30]. Therefore, thorough experiments are necessary to assess their safety and efficacy before widespread application. Here, we aimed to evaluate the potential roles of n-HAP and Fe_3O_4 NPs on bamboo plants under Cd toxicity, a concept that has not been extensively studied. The goal was to assess the potential of these NPs for environmental pollution removal and to improve bamboo plant tolerance to Cd. We hypothesize that foliar application of n-HAP and Fe_3O_4 NPs will reduce ROS levels in bamboo plants and increase bamboo plant tolerance under cadmium, with a positive impact on increasing antioxidant capacity, secondary metabolism, and water balance.

Bamboo, particularly species from the *Bambusoideae* subfamily, is known for its fast growth and high biomass, which makes it an ideal candidate for phytoremediation [31–33]. Bamboo species, due to their rapid vegetative growth and high biomass, are also capable of extracting metal ions through their roots, which makes them an effective tool in phy-

to remediation [34]. Furthermore, ornamental bamboo species such as *Pleiblastus pygmaeus* have been used as pollution indicators in urban areas, helping to clean contaminated air and water [35,36]. This species, which came from Japan to China in the 20th century, grows well in a variety of soil conditions and has expanded widely, especially in Jiangsu province [37,38]. In areas like Jiangsu, the pollution of agricultural land and forestry soils with heavy metals, particularly Cd, became a growing concern due to anthropogenic activities [39]. This pollution not only affects soil health but also hampers bamboo development. Therefore, it is crucial to come up with organic, bio-nutrient-based, and environmentally friendly solutions to mitigate soil toxicity and enhance plant tolerance to Cd. Therefore, we explored the potential of n-HAP and Fe₃O₄ NPs to promote bamboo plant tolerance under Cd toxicity. Specifically, we aimed to detect the effects of these NPs on Cd uptake, accumulation, translocation, plant water content, and the activation of cellular defense. Thus, this study represents a novel approach to understanding how n-HAP and Fe₃O₄ NPs can be used to enhance bamboo plant resilience under Cd stress, potentially offering a solution for metal remediation for agricultural sustainability.

2. Materials and Methods

2.1. Growth Conditions

Bamboo species were grown in a greenhouse with 16 h of light (30 °C) and 8 h of darkness (22 °C), maintaining a relative humidity range of 69–79%. The growth medium consisted of a mixture of coco peat and perlite in a 2:1 ratio, and the bamboo plants were cultivated in 3L pots. The plant species used in the experiment was *Pleiblastus pygmaeus*, a one-year-old bamboo species sourced from the Bamboo Research Institute at Nanjing Forestry University, Jiangsu, China, which was started in March 2024. The bamboo plants were grown for 60 days. Each pot contained five bamboo plants, and the study included five different Cd concentrations applied through irrigation: 0 (control), 50, 80, 100, and 150 mg L⁻¹. The total volume for each pot was 250 mL, with four replicates for each treatment during the experimental period. The design is shown in Table 1.

Table 1. The experimental design.

Treatments	Content of Treatments	Label
Control	0	A
Cd	50 mg L ⁻¹	B
Cd	80 mg L ⁻¹	C
Cd	100 mg L ⁻¹	D
Cd	150 mg L ⁻¹	E
Fe ₃ O ₄ NPs + Cd	100 mg L ⁻¹ Fe ₃ O ₄ NPs + 0 mg L ⁻¹ Cd	F
Fe ₃ O ₄ NPs + Cd	100 mg L ⁻¹ Fe ₃ O ₄ NPs + 50 mg L ⁻¹ Cd	G
Fe ₃ O ₄ NPs + Cd	100 mg L ⁻¹ Fe ₃ O ₄ NPs + 80 mg L ⁻¹ Cd	H
Fe ₃ O ₄ NPs + Cd	100 mg L ⁻¹ Fe ₃ O ₄ NPs + 100 mg L ⁻¹ Cd	I
Fe ₃ O ₄ NPs + Cd	100 mg L ⁻¹ Fe ₃ O ₄ NPs + 150 mg L ⁻¹ Cd	J
n-HAP + Cd	100 mg L ⁻¹ n-HAP + 0 mg L ⁻¹ Cd	K
n-HAP + Cd	100 mg L ⁻¹ n-HAP + 50 mg L ⁻¹ Cd	L
n-HAP + Cd	100 mg L ⁻¹ n-HAP + 80 mg L ⁻¹ Cd	M
n-HAP + Cd	100 mg L ⁻¹ n-HAP + 100 mg L ⁻¹ Cd	N
n-HAP + Cd	100 mg L ⁻¹ n-HAP + 150 mg L ⁻¹ Cd	O
n-HAP + Fe ₃ O ₄ NPs + Cd	100 mg L ⁻¹ n-HAP + Fe ₃ O ₄ NPs + 0 mg L ⁻¹ Cd	P
n-HAP + Fe ₃ O ₄ NPs + Cd	100 mg L ⁻¹ n-HAP + Fe ₃ O ₄ NPs + 50 mg L ⁻¹ Cd	Q
n-HAP + Fe ₃ O ₄ NPs + Cd	100 mg L ⁻¹ n-HAP + Fe ₃ O ₄ NPs + 80 mg L ⁻¹ Cd	R
n-HAP + Fe ₃ O ₄ NPs + Cd	100 mg L ⁻¹ n-HAP + Fe ₃ O ₄ NPs + 100 mg L ⁻¹ Cd	S
n-HAP + Fe ₃ O ₄ NPs + Cd	100 mg L ⁻¹ n-HAP + Fe ₃ O ₄ NPs + 150 mg L ⁻¹ Cd	T

n-HAP was obtained from Nanjing Jiancheng Company, Nanjing, China, with an average particle size of 60–80 nm, whilst Fe₃O₄ NPs were also supplied by Nanjing Jiancheng Company, with an average size of 20–30 nm. Fifty milligrams of n-HAP was dissolved in 500 mL of water, and the resultant solution was sprayed onto the bamboo leaves 20 days post-initiation of the trials. The application was repeated after 40 days, yielding a total concentration of 100 mg L⁻¹ n-HAP. Fe₃O₄ NPs were utilized according to a comparable methodology. The combination treatment involved an initial spray of 25 mg of n-HAP and 25 mg of Fe₃O₄ NPs, dissolved in 500 mL of water, administered to the bamboo leaves 20 days post-experiment initiation. The procedure was repeated after 40 days, yielding a cumulative concentration of 100 mg L⁻¹ n-HAP + Fe₃O₄ NPs. A 400 mL nutritional solution was administered to each pot every five days. Photosynthetic and morphological characteristics were observed in the greenhouse. The roots, leaves, and stems were individually harvested, sampled, and transported to the lab. The samples were preserved in a Haier–China refrigerator for subsequent investigation of biochemical indices.

2.2. Determination of Biochemical Indexes

To prepare the sample, bamboo leaves (0.6 g) were crushed in liquid nitrogen. A total of 4 mg of pH 7.6 buffer (phosphate) was then mixed to the leaf powders. To obtain the final supernatant, the mixture was centrifuged at 4500–5500 × g at 6 °C for 15 min, which was used for measuring biochemical parameters.

Superoxide dismutase (SOD) activity was determined by the method of Senthilkumar et al. (2002) [40], which was nitro blue tetrazolium photoreduction. The activity of phenylalanine ammonia-lyase (PAL) was measured as per the Berner protocol [41] and expressed as U mg⁻¹ of protein. The activities of catalase (CAT), glutathione reductase (GR), and peroxidase (POD) were assessed using the methods of Aebi (1984) [42], Liu et al. (2014) [43], and Foyer and Halliwell (1976) [44], with certain modifications. The glyoxalase (Gly I) activity was determined according to the method of Hasanuzzaman et al. (2011) [45], which necessitates recording absorbance in 240 nm wavelengths for 1 min. Gly II activity was determined by Principato et al.'s (1987) [46] methodology. Extracts of protein were measured at a 412 nm wavelength for 1 min. The methylglyoxal (MG) content was measured using the protocol by Yadav et al. (2005) [47]. The reprivatized MG was obtained by recording absorbance in the 200–500 nm wavelength range for 17 cycles, each separated by 1 min intervals. The reference method from McDonald and Prenzler (2001) [48] was used for calculating the total phenolic content (TPC). Folin–Ciocalteu reagent was applied, and gallic acid was used as a standard. Total flavonoid content (TFC) was measured according to the protocol of Chang et al. (2002) [49], utilizing a quercetin standard to construct the calibration curve. The content of malondialdehyde (MDA) was determined as per Rao and Sresty method [50]. ROS components including hydrogen peroxide (H₂O₂) and superoxide radical (O₂•⁻) content were measured by the method of Velikova et al. (2000) [51]. We used Valentovic et al.'s (2006) [52] approaches to measure electrolyte leakage (EL), which showed the difference between the primary and final electrical conductivities (EC₁) and (EC₂). To find the EL percentage, the following method was used:

$$\text{EL (\%)} = (\text{EC}_1 / \text{EC}_2) \times 100$$

2.3. Determination of Physiological Indexes

Proline accumulation was measured by using a standard method (Bates et al., 1973) [53]. The content of nitric oxide was measured by a detection kit which was purchased from Solar Bio Life Science, Beijing, China. RWC was calculated based on the protocol of Dhopte and Manuel (2002) [54], in which RWC was obtained by measurement of saturation

weight (SW), fresh weight (FW) (in leaves immersed in distilled water o/n), and dry weight (DW) (at 70 °C o/n) according to the following formula:

$$\text{RWC (\%)} = (\text{FW} - \text{DW}) / (\text{SW} - \text{DW}) \times 100$$

The total photosynthetic pigments were measured by using the protocol of Arnon (1949) [55]. In total, 100 mg of leaf extract was added to 80% acetone and centrifuged at 8000 rpm for 10 min. The amount of total chlorophyll absorbed in 630, 647, and 664 nm was measured by a spectrophotometer (Hitachi U-2001, Tokyo, Japan). To measure gas exchange, we examined the intercellular net photosynthesis (P_n), the CO₂ content (C_i), and the stomatal conductance (G_s) by a portable gas exchange device on larger leaves at 26 °C at 9:30 in the morning (Holá et al., 2010) [56].

2.4. Determination of Biomass Indexes

After the experiment was over, the roots and shoots of bamboo were carefully washed and cleaned. The samples were dried in a vacuum-drying oven (DZF-6090, Xiamen Tob New Energy Technology, Xiamen, China) at 118 °C for 30 min to remove the water. After being put in an oven at 78 °C for 48 h, the samples were incubated until their weight remained constant. The root and shoot samples were dried out and then weighed for all four replicates, and this was recorded as the root and shoot dry weight.

2.5. Accumulation of Cd in Bamboo Organs (Shoot, Roots, and Stems)

For measurement of Cd content, dry leaf samples of plants (0.5 g) were added to 6 mL of nitric acid (HNO₃-64%), and then the mixture was incubated overnight (o/n) at 28 °C. Then, the mixture was transferred to an oven (China Energy) at a temperature of 95 °C, which led to the evaporation of all the NO₂. The content of Cd in all plant organs was measured by applying an ICP-MS (Agilent 4500 series, Webster, MA, USA) procedure (Khosropour et al., 2019) [57].

2.6. Calculation of the Translocation Factor, Bioaccumulation Factor, and Tolerance Index

The translocation factor (TF), bioaccumulation factor (BAF), and tolerance index (TI) were phyto-extraction efficiency indicators calculated by using the protocol of Sourti and Karimi [58] that demonstrate the phytoremediation capacity of bamboo plants for Cd. The values of TF, BAF, and TI were computed using the subsequent formula:

$$\text{TF} = (\text{Cd accumulation in the leaves and stem}) / (\text{Cd accumulation in the root})$$

$$\text{BAF} = (\text{Cd accumulation in leaves, root, and stem}) / (\text{Cd accumulation in the medium})$$

$$\text{TI of root} = (\text{Cd in root dry weight}) / (\text{root dry weight of control})$$

$$\text{TI of Shoot} = (\text{Cd in shoot dry weight}) / (\text{shoot dry weight of control})$$

2.7. Statistical Analysis

The data collected in this study were analyzed using R free software, employing a two-way factorial design. The treatments were arranged in a completely randomized design (CRD) with four replicates (n = 4). Mean difference computation among treatments was analyzed with Duncan's test at a level of $p < 0.05$.

3. Results

3.1. Biochemical Indexes

3.1.1. Antioxidant Enzyme Activity

The data analysis of antioxidant activity revealed significant differences between treatments in the stimulation of antioxidant enzymes such as SOD, POD, CAT, GR, and PAL ($p < 0.001$). The results indicated that the addition of n-HAP and Fe₃O₄ NPs significantly enhanced the antioxidant capacity of bamboo plants. As shown in Figure 1, the highest increases in antioxidant activity were observed with the combination of 100 mg L⁻¹ n-HAP + Fe₃O₄, 100 mg L⁻¹ n-HAP, and 100 mg L⁻¹ Fe₃O₄ NPs, with a 100%, 86%, and 75% increase in SOD activity, a 51%, 42%, and 36% increase in POD activity, a 65%, 59%, and 52% increase in CAT activity, a 57%, 49%, and 42% increase in GR activity, and a 61%, 50%, and 43% increase in PAL activity, respectively. Furthermore, the results demonstrated that antioxidant activity increased under Cd stress, with the highest levels associated with the combination of 100 mg L⁻¹ n-HAP + Fe₃O₄ under 50 and 80 mg L⁻¹ Cd. This combination led to a 63% and 58% increase in SOD activity, a 30% and 25% increase in POD, a 44% and 39% increase in CAT, a 33% and 29% increase in GR, and a 36% and 27% increase in PAL activity compared to the control treatments, respectively. Additionally, the combination of 100 mg/L n-HAP + Fe₃O₄ increased antioxidant activity in bamboo plants under all four concentrations of Cd (50, 80, 100, and 150 mg L⁻¹), while similar results were observed under 50 and 80 mg L⁻¹ Cd with the individual addition of n-HAP and Fe₃O₄ (Figure 1).

3.1.2. Glyoxalase Activity

The data showed a significant difference in the glyoxalase activity of bamboo species under various Cd levels ($p < 0.001$). It was observed that the addition of n-HAP and Fe₃O₄, both individually and in combination, resulted in increased glyoxalase activity, GlyI, and GlyII (Figure 2). The greatest enhancement in glyoxalase activity under Cd stress was associated with the combination of 100 mg L⁻¹ n-HAP + Fe₃O₄ at 50 and 80 mg L⁻¹ Cd, as well as with 100 mg L⁻¹ n-HAP at 50 mg L⁻¹ Cd, showing a 21%, 17%, and 16% increase in GlyI activity and a 44%, 37%, and 31% increase in GlyII activity, respectively, compared to respective controls. Furthermore, a significant difference was found between treatments in the content of methylglyoxal (MG). The addition of n-HAP and Fe₃O₄, both individually and in combination, led to a reduction in MG content in Cd-stressed bamboo plants as compared to the controls ($p < 0.001$). The most substantial reduction in MG was observed with the combination of 100 mg L⁻¹ n-HAP + Fe₃O₄ under 50 mg L⁻¹ Cd, showing a 21% decrease in MG content.

3.1.3. Plant Secondary Metabolism

The results revealed significant differences among the various treatments for both TFC and TPC ($p < 0.001$). While different levels of Cd negatively affected the stimulation of non-antioxidant enzyme activity, the addition of n-HAP and Fe₃O₄ NPs significantly enhanced TFC and TPC in bamboo species under Cd stress (Figure 3). The highest increase in non-antioxidant molecules was observed with the combination of 100 mg L⁻¹ n-HAP and Fe₃O₄ NPs under 50 and 80 mg L⁻¹ Cd, showing a 37% and 31% increase in TFC and a 36% and 29% increase in TPC, respectively, compared to their respective control groups.

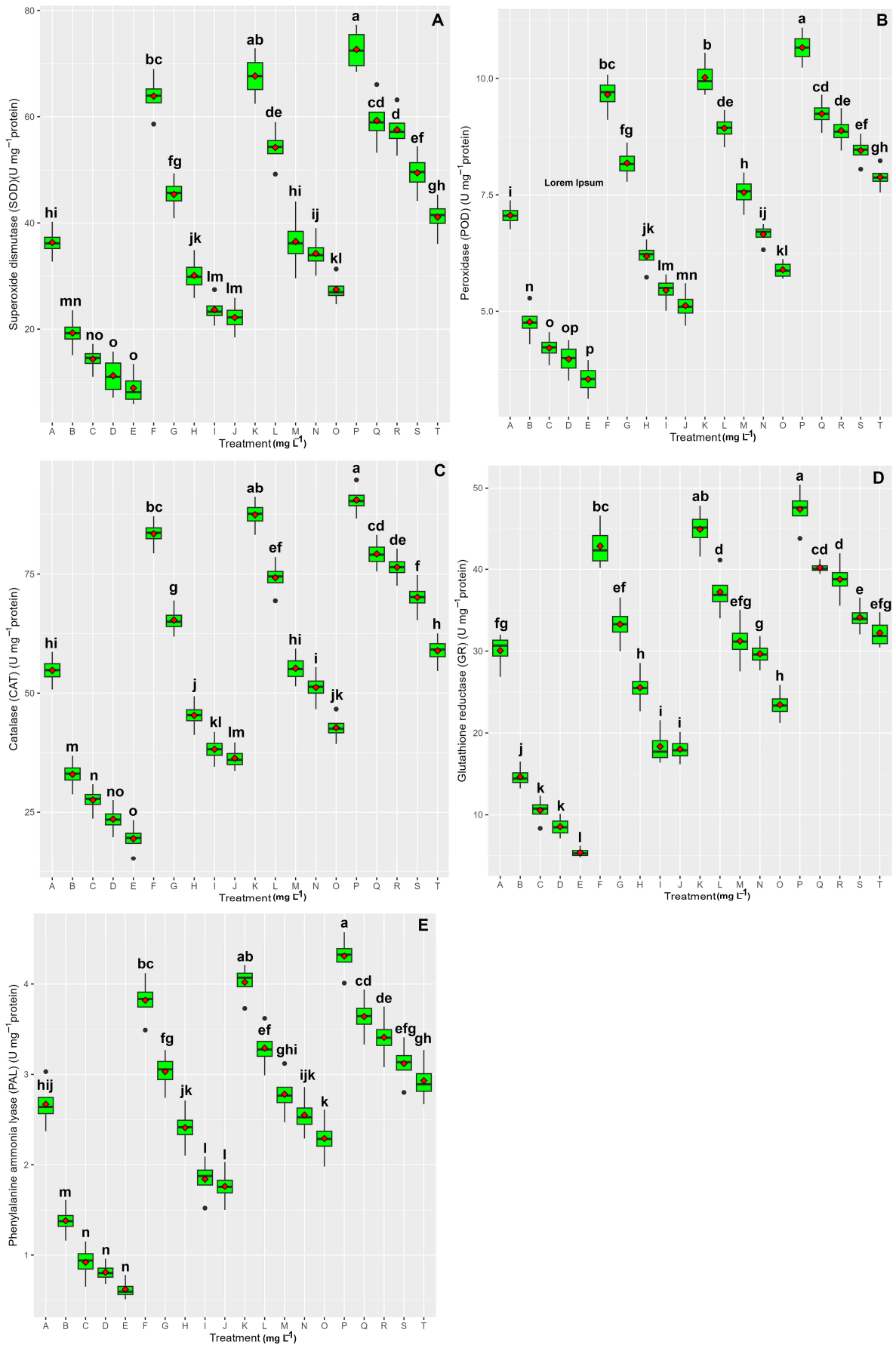


Figure 1. The impact of n-HAP and Fe₃O₄ NPs, both individually and in combination, at varying concentrations of Cd on antioxidant enzyme activity: (A) superoxide dismutase (SOD); (B) peroxidase

(POD); (C) catalase (CAT); (D) glutathione reductase (GR); and (E) phenylalanine ammonia-lyase (PAL). The whiskers represent 1.5 times the interquartile range below the first quartile and above the third quartile, with dots indicating outliers. The lines within the boxes denote the median values, while the red diamonds indicate the means. Lowercase letters indicate significant differences among treatments based on Duncan's test ($p < 0.05$). Treatments are labeled A through T on the horizontal axis; detailed information is provided in Table 1.

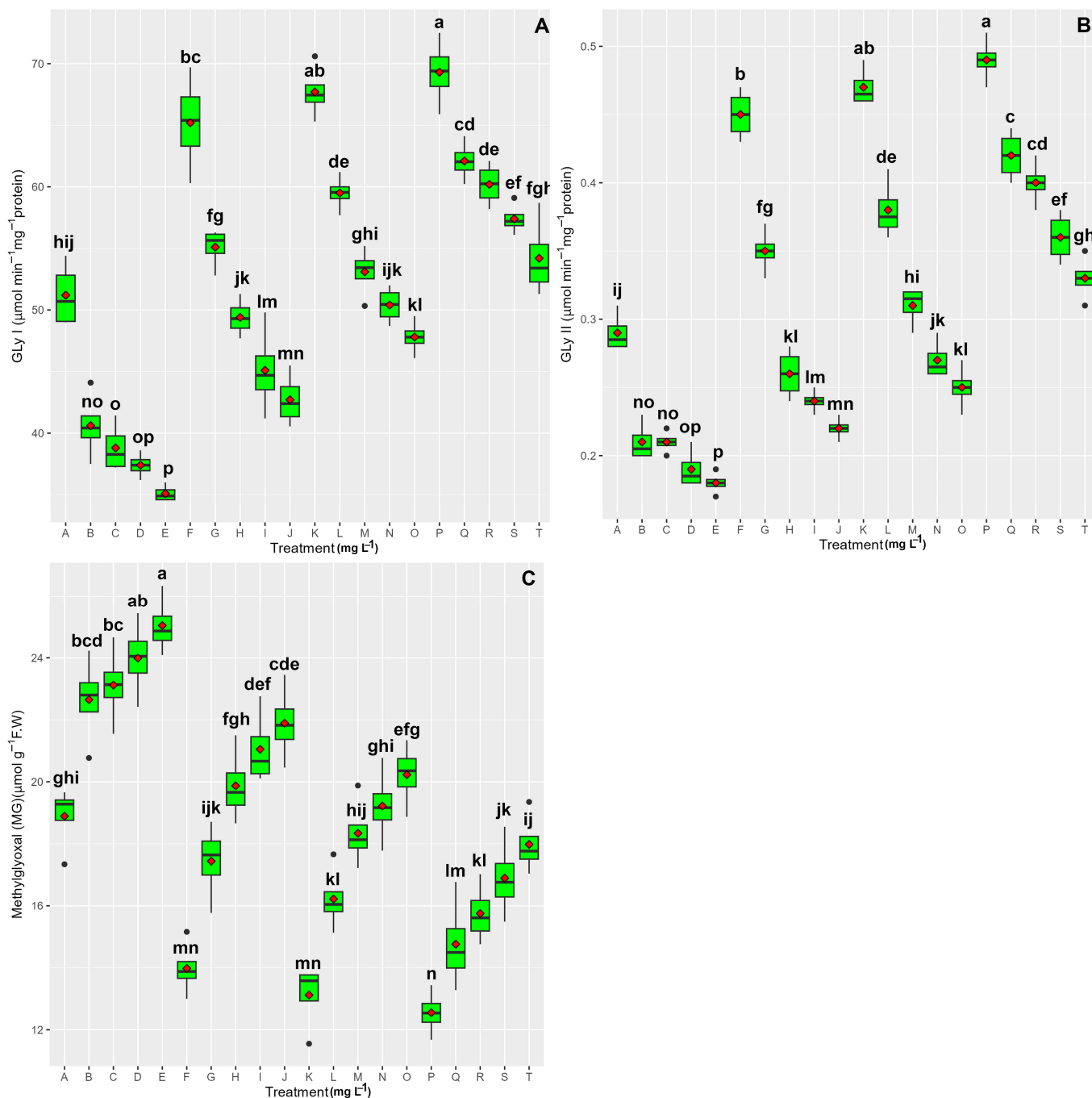


Figure 2. The impact of n-HAP and Fe_3O_4 NPs, both individually and in combination, at varying concentrations of Cd on GLyI (A), GLyII (B), and MG (C). The whiskers represent 1.5 times the interquartile range below the first quartile and above the third quartile, with dots indicating outliers. The lines within the boxes denote the median values, while the red diamonds indicate the means. Lowercase letters indicate significant differences among treatments based on Duncan's test ($p < 0.05$). Treatments are labeled A through T on the horizontal axis; detailed information is provided in Table 1.

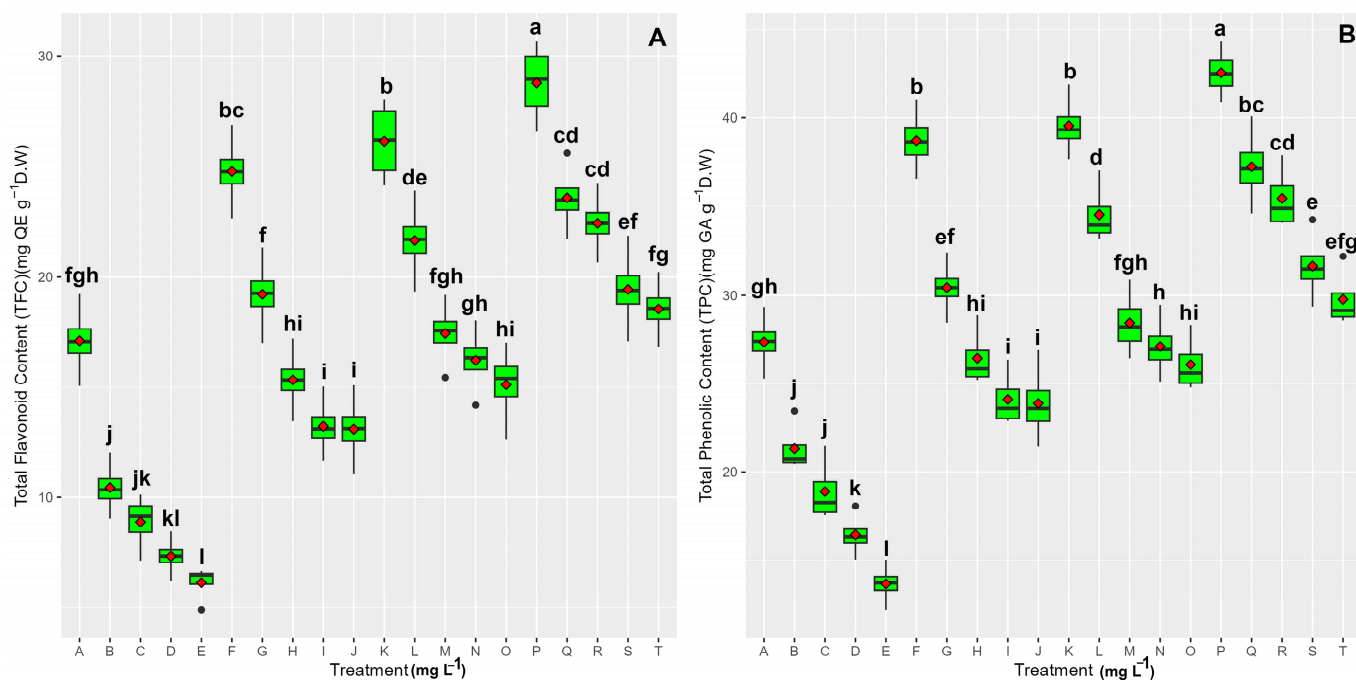


Figure 3. The impact of n-HAP and Fe₃O₄ NPs, both individually and in combination, at varying concentrations of Cd on TFC (A) and TPC (B). The whiskers represent 1.5 times the interquartile range below the first quartile and above the third quartile, with dots indicating outliers. The lines within the boxes denote the median values, while the red diamonds indicate the means. Lowercase letters indicate significant differences among treatments based on Duncan's test ($p < 0.05$). Treatments are labeled A through T on the horizontal axis; detailed information is provided in Table 1.

3.1.4. Plant Oxidative Indexes

The results indicated one significant reduction with the addition of 100 mg L⁻¹ n-HAP and 100 mg L⁻¹ Fe₃O₄ in H₂O₂, O₂, MDA, and EL in bamboo species under Cd stress ($p < 0.001$). Specifically, the highest reduction occurred with the combination of 100 mg L⁻¹ n-HAP and Fe₃O₄ under 50 mg L⁻¹ Cd, where H₂O₂ levels decreased by 39%, O₂ by 56%, MDA by 45%, and the levels of EL by 62%. Moreover, the results demonstrated that the treatments combining 100 mg L⁻¹ n-HAP and Fe₃O₄ were more effective in reducing oxidative stress and mitigating cell membrane injury in bamboo plants across all Cd concentrations (50, 80, 100, and 150 mg L⁻¹) (Figure 4).

3.1.5. Plant Physiological Indexes

Nitric Oxide Content, Proline Accumulation, and RWC

A substantial disparity emerged among the different treatments for nitric oxide levels, proline accumulation, and RWC across the groups ($p < 0.001$) (Figure 5). The results indicated that exposure to different concentrations of Cd (50, 80, 100, and 150 mg L⁻¹) led to an imbalance in the physiology of bamboo plants, with a 33%, 42%, 48%, and 59% decrease in nitric oxide content, a 35%, 41%, 50%, and 57% decrease in proline, and a 37%, 49%, 55%, and 62% reduction in RWC; 100 mg L⁻¹ n-HAP and Fe₃O₄ effectively increased these physiological indices. Specifically, nitric oxide content increased by 58%, 50%, 32%, and 11%, proline accumulation increased by 51%, 43%, 23%, and 13%, and RWC increased by 39%, 32%, 21%, and 11% under 50, 80, 100, and 150 mg L⁻¹ Cd, respectively (Figure 5).

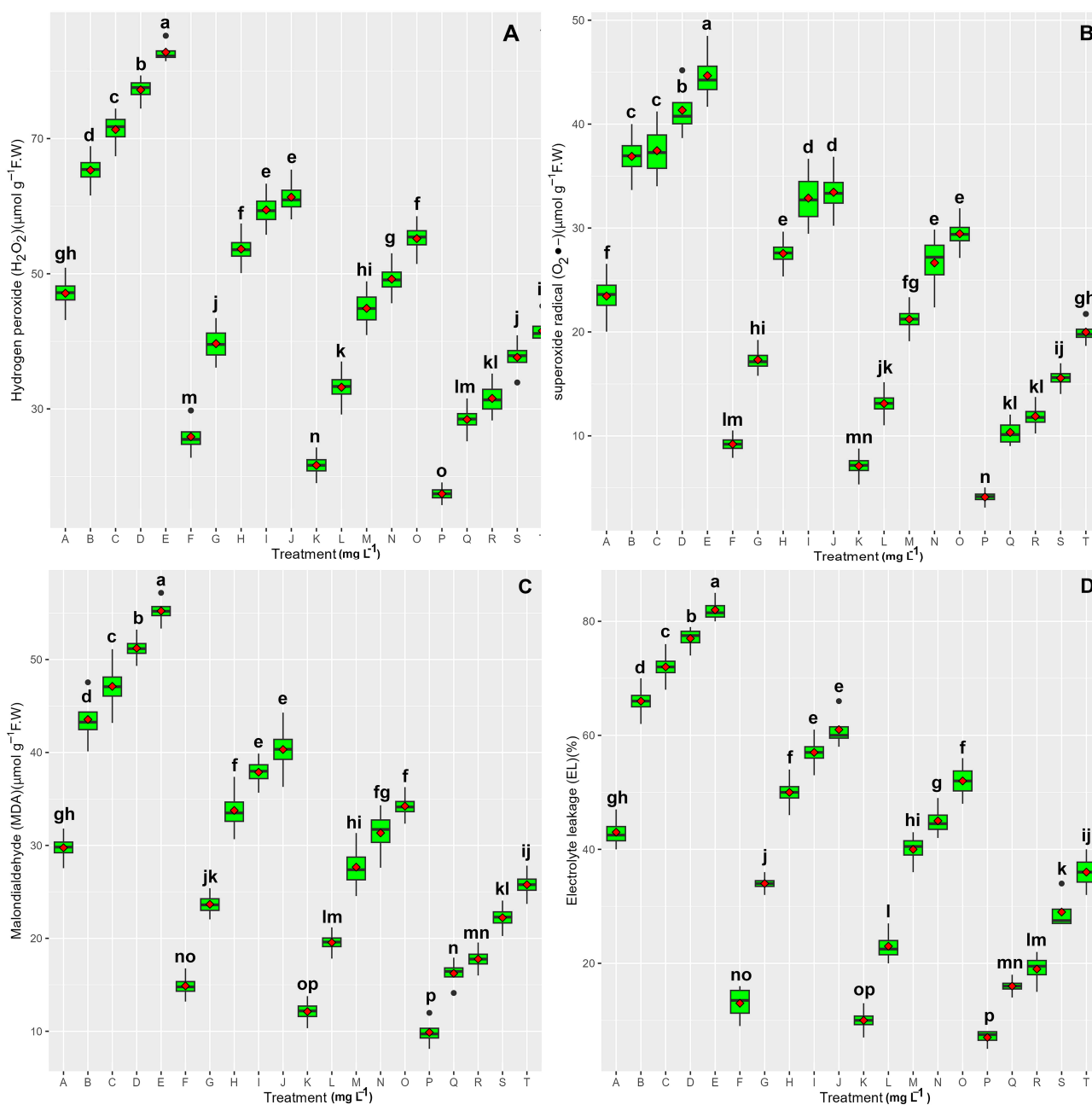


Figure 4. The impact of n-HAP and Fe_3O_4 NPs, both individually and in combination, at varying concentrations of Cd on hydrogen peroxide (H_2O_2) (A), superoxide radical ($\text{O}_2\bullet^-$) (B), malondialdehyde (MDA) (C), and electrolyte leakage (EL) (D). The whiskers represent 1.5 times the interquartile range below the first quartile and above the third quartile, with dots indicating outliers. The lines within the boxes denote the median values, while the red diamonds indicate the means. Lowercase letters indicate significant differences among treatments based on Duncan's test ($p < 0.05$). Treatments are labeled A through T on the horizontal axis; detailed information is provided in Table 1.

Total Photosynthetic Pigments and Gaseous Exchange

The measurement of photosynthetic properties, encompassing total chlorophyll, intercellular net photosynthesis (P_n), intercellular CO_2 concentration (C_i), and stomata conductance (G_s), demonstrated significant differences across treatments for photosynthetic pigments and gas exchange parameters ($p < 0.001$). Exposure to Cd diminished photosynthetic efficiency, according to reduced photosynthetic quality indicators; however, the incorporation of n-HAP and Fe_3O_4 significantly enhanced bamboo plant photosynthesis under Cd stress. Significant enhancements were found with the combination of 100 mg L^{-1}

n-HAP and Fe₃O₄ at 50 and 80 mgL⁻¹ Cd, exhibiting a 27% and 21% growth in total chlorophyll content, a 32% and 26% rise in Pn, a 29% and 24% increase in Ci, and a 48% and 44% increase in the level in Gs relative to controls, respectively. The findings indicate that the incorporation of n-HAP and Fe₃O₄, both separately and together, can enhance the photosynthetic capability of bamboo plants. However, the combination form was much more effective in boosting bamboo plant photosynthesis under different concentrations of Cd (Figure 6).

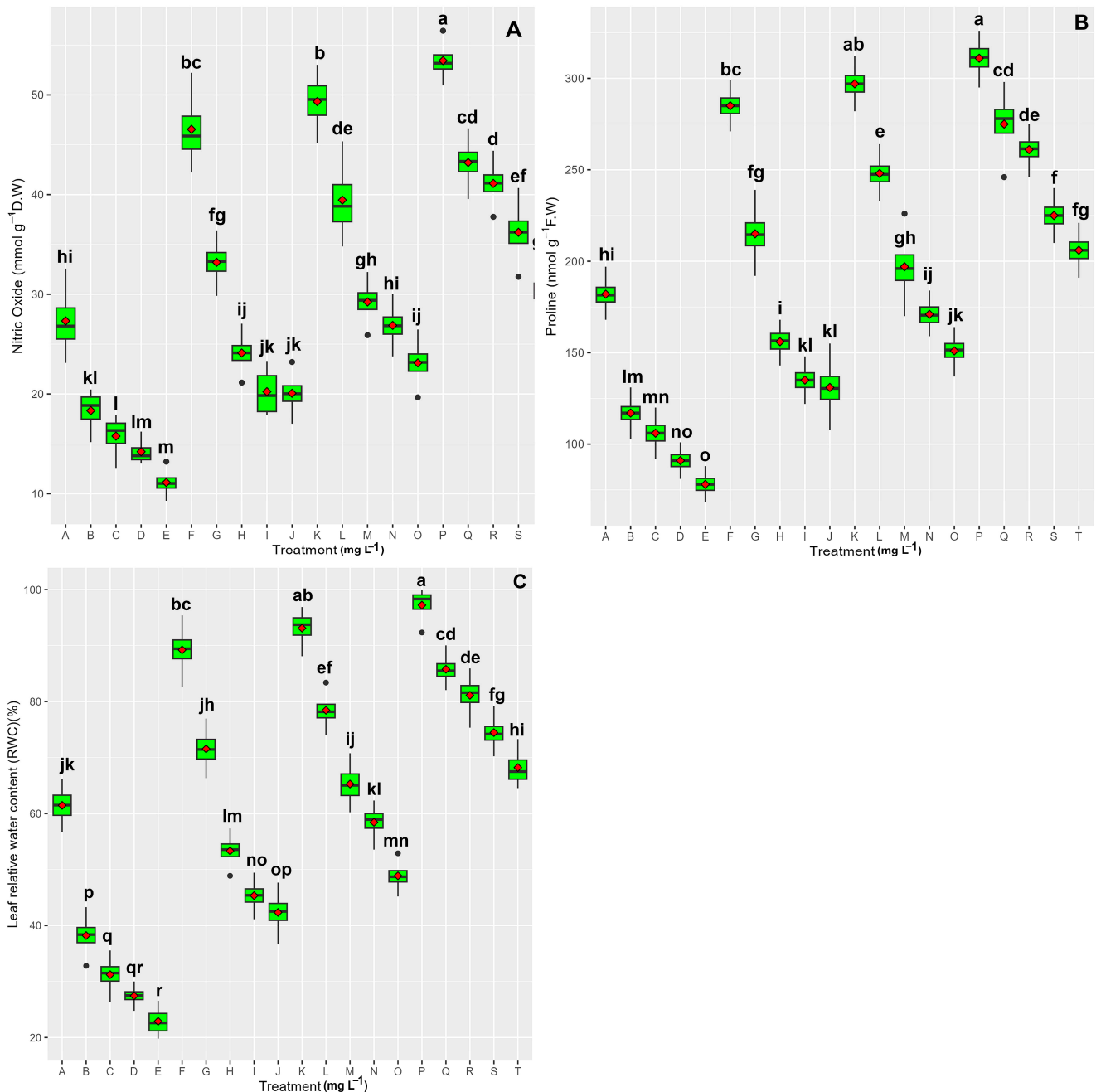


Figure 5. The impact of n-HAP and Fe₃O₄ NPs, both individually and in combination, at varying concentrations of Cd on nitric oxide (A), proline accumulation (B), and relative water content (RWC) (C). The whiskers represent 1.5 times the interquartile range below the first quartile and above the third quartile, with dots indicating outliers. The lines within the boxes denote the median values, while the red diamonds indicate the means. Lowercase letters indicate significant differences among treatments based on Duncan's test ($p < 0.05$). Treatments are labeled A through T on the horizontal axis; detailed information is provided in Table 1.

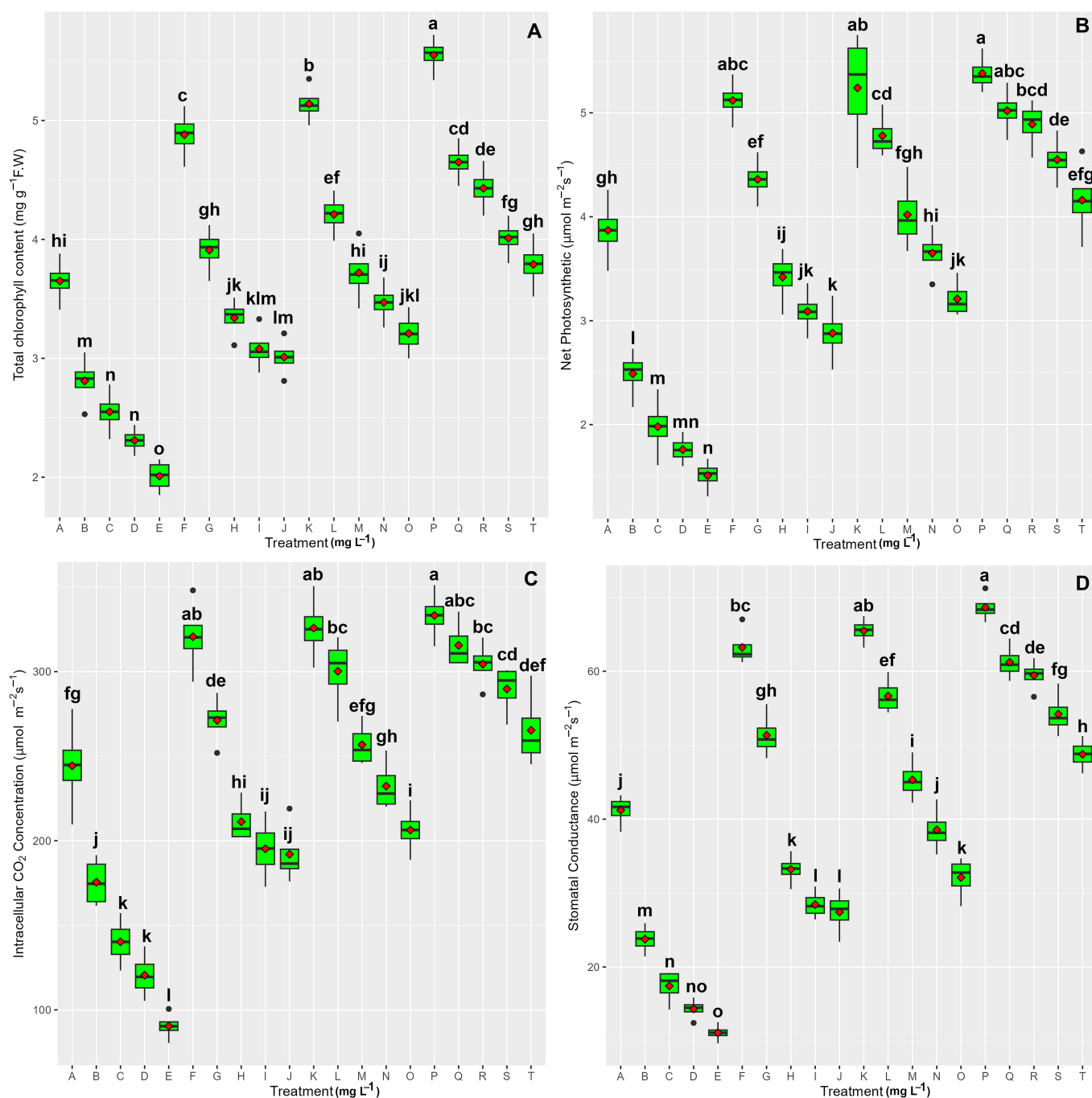


Figure 6. The impact of n-HAP and Fe_3O_4 NPs, both individually and in combination, at varying concentrations of Cd on total chlorophyll (T-Chl) (A), intercellular net photosynthesis (Pn) (B), intercellular CO_2 concentration (C_i) (C), and stomata conductance (G_s) (D). The whiskers represent 1.5 times the interquartile range below the first quartile and above the third quartile, with dots indicating outliers. The lines within the boxes denote the median values, while the red diamonds indicate the means. Lowercase letters indicate significant differences among treatments based on Duncan's test ($p < 0.05$). Treatments are labeled A through T on the horizontal axis; detailed information is provided in Table 1.

Biomass Indexes

The results derived from the biomass indices, encompassing root and shoot dry weight, revealed considerable variation ($p < 0.001$) between treatments (Figure 7). Exposure to Cd concentrations of 50, 80, 100, and 150 mgL^{-1} led to a significant reduction in biomass indices, with a 24%, 32%, 37%, and 44% decrease in shoot dry weight and a 24%, 31%, 38%,

and 41% decrease in root dry weight, respectively. However, the addition of 100 mgL⁻¹ n-HAP and 100 mgL⁻¹ Fe₃O₄ notably promoted both shoot and root dry weight. The most significant increase in biomass indexes was observed with the combination of n-HAP and Fe₃O₄ under 50 and 80 mgL⁻¹ Cd, showing a 29% and 27% increase in root dry weight and a 26% and 22% increase in shoot dry weight, respectively. The percentage of increase and decrease in biomass relative to the control treatments (without Cd and nanoparticles) is presented in Table 2.

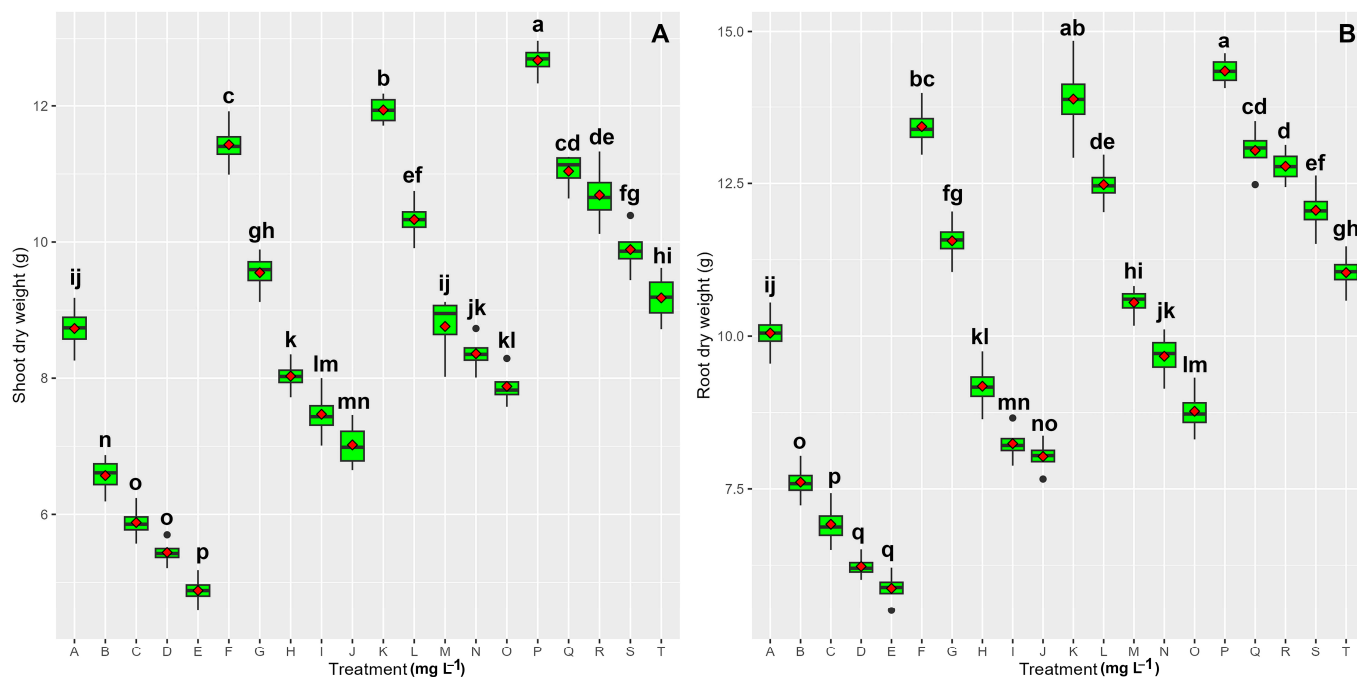


Figure 7. The impact of n-HAP and Fe₃O₄ NPs, both individually and in combination, on different levels of Cd on shoot dry weight (SHDW) (A) and root dry weight (RDW) (B). The whiskers represent 1.5 times the interquartile range below the first quartile and above the third quartile, with dots indicating outliers. The lines within the boxes denote the median values, while the red diamonds indicate the means. Lowercase letters indicate significant differences among treatments based on Duncan’s test ($p < 0.05$). Treatments are labeled A through T on the horizontal axis; detailed information is provided in Table 1.

Table 2. The effects of n-HAP and Fe₃O₄ NPs alone and in combination at different Cd concentrations on root dry weight (RDW), and shoot dry weight (SHDW) in *Pleioblastus pygmaea* L. compared to control treatment. ↑ and ↓ signify increase and decrease, respectively.

Treatments (mg L ⁻¹)	Cd (mg L ⁻¹)	RDW (%)	SHDW (%)
100 mg L ⁻¹ n-HAP	0 mg L ⁻¹	38% ↑	36% ↑
100 mg L ⁻¹ Fe ₃ O ₄ NPs	0 mg L ⁻¹	33% ↑	31% ↑
100 mg L ⁻¹ n-HAP + Fe ₃ O ₄ NPs	0 mg L ⁻¹	42% ↑	45% ↑
50 mg L ⁻¹ Cd	50 mg L ⁻¹	24% ↓	24% ↓
100 mg L ⁻¹ n-HAP	50 mg L ⁻¹	24% ↑	18% ↑
100 mg L ⁻¹ Fe ₃ O ₄ NPs	50 mg L ⁻¹	15% ↑	9% ↑
100 mg L ⁻¹ n-HAP + Fe ₃ O ₄ NPs	50 mg L ⁻¹	29% ↑	26% ↑
80 mg L ⁻¹	80 mg L ⁻¹	31% ↑	32% ↓
100 mg L ⁻¹ n-HAP	80 mg L ⁻¹	5% ↑	1% ↑
100 mg L ⁻¹ Fe ₃ O ₄ NPs	80 mg L ⁻¹	8% ↓	8% ↓
100 mg L ⁻¹ n-HAP + Fe ₃ O ₄ NPs	80 mg L ⁻¹	27% ↑	22% ↑
100 mg L ⁻¹	100 mg L ⁻¹	38% ↓	37% ↓
100 mg L ⁻¹ n-HAP	100 mg L ⁻¹	3% ↓	4% ↓

Table 2. Cont.

Treatments (mg L ⁻¹)	Cd (mg L ⁻¹)	RDW (%)	SHDW (%)
100 mg L ⁻¹ Fe ₃ O ₄ NPs	100 mg L ⁻¹	18% ↓	14% ↓
100 mg L ⁻¹ n-HAP + Fe ₃ O ₄ NPs	100 mg L ⁻¹	20% ↑	13% ↑
100 mg L ⁻¹	150 mg L ⁻¹	41% ↓	44% ↓
100 mg L ⁻¹ n-HAP	150 mg L ⁻¹	12% ↓	9% ↓
100 mg L ⁻¹ Fe ₃ O ₄ NPs	150 mg L ⁻¹	20% ↓	19% ↓
100 mg L ⁻¹ n-HAP + Fe ₃ O ₄ NPs	150 mg L ⁻¹	9% ↑	5% ↑

3.1.6. Cd Accumulation

The data on Cd content in bamboo organs revealed significant differences across treatments in the levels of Cd in the leaves, roots, and stems ($p < 0.001$): 100 mgL⁻¹ n-HAP and 100 mgL⁻¹ Fe₃O₄ markedly decreased Cd accumulation in bamboo plants. The highest reduction in Cd was observed with the combination of 100 mgL⁻¹ n-HAP and 100 mgL⁻¹ Fe₃O₄ under 50 mgL⁻¹ Cd and 80 mgL⁻¹ Cd, resulting in reductions of 72% and 64% in the bamboo leaves, 58% and 57% in the stems, and 62% and 54% in the roots, respectively (Figure 8).

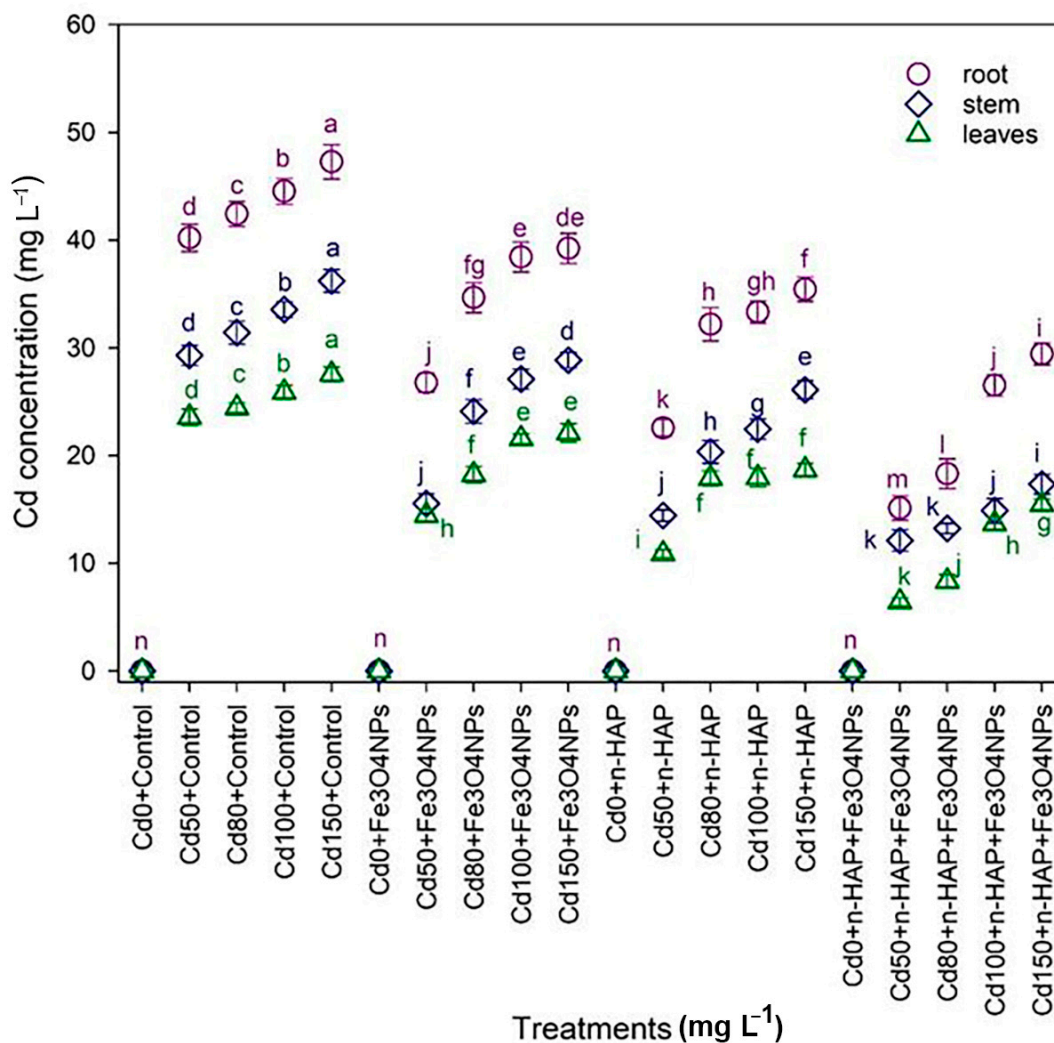


Figure 8. The accumulation of Cd (mg L⁻¹) in different parts of the bamboo species exposed to different Cd levels. Different lowercase letters indicate significant differences between different treatments in organs. Colors show the comparison between groups in the organs in Duncan’s test ($p < 0.05$).

3.1.7. Plant Tolerance Indexes

We calculated the Plant Tolerance Index (TI), the translocation factor (TF), and the bioaccumulation factor (BAF) to assess how bamboo reacts to different levels of Cd stress. Significant differences in TF and BAF were observed across treatments ($p < 0.001$). The most substantial reduction in both TF and BAF occurred with the combination of 100 mgL⁻¹ n-HAP and Fe₃O₄ under 50 mgL⁻¹ Cd exposure. Specifically, TF in the leaves and stems was reduced by 31% and 35%, respectively, while BAF in the leaves, stems, and roots decreased by 87%, 87%, and 81%, respectively, compared to the controls. Other treatments, both single and combined, also led to significant reductions in TF and BAF. These included the following combinations: 100 mgL⁻¹ n-HAP + Fe₃O₄ + 80 mgL⁻¹ Cd, 100 mgL⁻¹ n-HAP + 50 mgL⁻¹ Cd, and 100 mgL⁻¹ Fe₃O₄ + 50 mgL⁻¹ Cd. These treatments resulted in reductions in TF ranging from 16% to 32% in leaves and stems and 45% to 81% in roots. Similarly, reductions in BAF ranged from 65% to 82% in the leaves, 61% to 75% in the stems, and 45% to 79% in the roots. The addition of NPs significantly enhanced the bamboo plants' tolerance to Cd stress, as shown by the increase in TI. The combination of 100 mgL⁻¹ n-HAP and Fe₃O₄ under 50 and 80 mgL⁻¹ Cd resulted in the highest increase in TI, with 22% and 18% increases in TI for the shoot and 23% and 21% increases in TI for the root, respectively. In contrast, individual treatments with 100 mgL⁻¹ n-HAP and 100 mgL⁻¹ Fe₃O₄ under 50 mgL⁻¹ Cd showed moderate increases in TI, with 14% and 5% increases in TI for the shoots and 18% and 9% increases in TI for the roots, respectively, compared to the controls (Table 3). The application of NPs, particularly the combination of 100 mgL⁻¹ n-HAP and Fe₃O₄, significantly reduced Cd translocation and bioaccumulation while enhancing the bamboo plants' tolerance, as indicated by the increased TI.

Table 3. Differences in shoot and root tolerance index (TI), bioaccumulation factor (BAF) of root, stem, and leaves, and translocation factor (TF) of leaves and stem for 0, 50, 80, 100, and 150 mg L⁻¹ Cd, under 100 mg L⁻¹ n-HAP, and 100 mg L⁻¹ Fe₃O₄ NPs. Different lowercase letters indicate significant differences between different treatments in organs. The data demonstrate the mean ± standard error (n = 4).

Treatments	TI (Root)	TI (Shoot)	TF (Leaf)	TF (Stem)	BAF (Leaf)	BAF (Stem)	BAF (Root)
0	1.00 ± 0.002 ^{gh}	1.00 ± 0.002 ^{hi}	0	0	0	0	0
100 mg L ⁻¹ n-HAP + 0 mg L ⁻¹ Cd	1.35 ± 0.002 ^a	1.32 ± 0.002 ^b	0	0	0	0	0
100 mg L ⁻¹ Fe ₃ O ₄ NPs + 0 mg L ⁻¹ Cd	1.27 ± 0.002 ^b	1.26 ± 0.002 ^{bc}	0	0	0	0	0
100 mg L ⁻¹ n-HAP + Fe ₃ O ₄ NPs + 0 mg L ⁻¹ Cd	1.42 ± 0.002 ^a	1.55 ± 0.002 ^a	0	0	0	0	0
100 mg L ⁻¹ n-HAP + 50 mg L ⁻¹ Cd	0.72 ± 0.002 ^{mn}	0.73 ± 0.005 ⁿ	0.57 ± 0.0006 ^{bcd}	0.73 ± 0.0005 ^{cd}	1.54 ± 0.001 ^d	1.73 ± 0.002 ^d	2.94 ± 0.008 ^d
100 mg L ⁻¹ Fe ₃ O ₄ NPs + 50 mg L ⁻¹ Cd	1.18 ± 0.002 ^{cd}	1.14 ± 0.002 ^{ef}	0.47 ± 0.0006 ^g	0.54 ± 0.0005 ^h	0.44 ± 0.001 ^l	0.50 ± 0.002 ^l	0.80 ± 0.008 ^{lm}
100 mg L ⁻¹ n-HAP + Fe ₃ O ₄ NPs + 50 mg L ⁻¹ Cd	1.09 ± 0.002 ^{ef}	1.35 ± 0.002 ^{gh}	0.52 ± 0.0006 ^{ef}	0.58 ± 0.0005 ^g	0.53 ± 0.001 ^k	0.67 ± 0.002 ^j	0.96 ± 0.008 ^{jk}
100 mg L ⁻¹ n-HAP + 80 mg L ⁻¹ Cd	0.65 ± 0.002 ^{no}	0.65 ± 0.005 ^o	0.58 ± 0.0006 ^{bc}	0.74 ± 0.0005 ^c	1.83 ± 0.001 ^c	2.02 ± 0.002 ^c	3.44 ± 0.008 ^c
100 mg L ⁻¹ Fe ₃ O ₄ NPs + 80 mg L ⁻¹ Cd	0.95 ± 0.002 ^{hi}	0.96 ± 0.005 ^{ij}	0.52 ± 0.0006 ^{ef}	0.63 ± 0.0005 ^f	0.68 ± 0.001 ⁱ	0.78 ± 0.002 ⁱ	1.32 ± 0.008 ⁱ
100 mg L ⁻¹ n-HAP + Fe ₃ O ₄ NPs + 80 mg L ⁻¹ Cd	0.87 ± 0.002 ^{jk}	0.88 ± 0.005 ^{kl}	0.53 ± 0.0006 ^{def}	0.69 ± 0.0005 ^e	0.93 ± 0.001 ^h	1.30 ± 0.002 ^g	1.66 ± 0.008 ^h
100 mg L ⁻¹ n-HAP + 100 mg L ⁻¹ Cd	1.21 ± 0.002 ^{bcd}	1.18 ± 0.002 ^{de}	0.44 ± 0.0006 ^h	0.50 ± 0.0005 ⁱ	0.34 ± 0.001 ^m	0.35 ± 0.002 ^m	0.86 ± 0.008 ^{kl}
100 mg L ⁻¹ Fe ₃ O ₄ NPs + 100 mg L ⁻¹ Cd	0.61 ± 0.002 ^{op}	0.59 ± 0.002 ^o	0.61 ± 0.0006 ^b	0.79 ± 0.0005 ^b	2.02 ± 0.001 ^b	2.44 ± 0.002 ^b	3.92 ± 0.008 ^b
100 mg L ⁻¹ n-HAP + Fe ₃ O ₄ NPs + 100 mg L ⁻¹ Cd	0.91 ± 0.002 ^{ij}	0.92 ± 0.005 ^{jk}	0.53 ± 0.0006 ^{def}	0.67 ± 0.0005 ^e	1.89 ± 0.001 ^h	1.12 ± 0.002 ^h	1.64 ± 0.008 ^h
100 mg L ⁻¹ n-HAP + 150 mg L ⁻¹ Cd	0.78 ± 0.002 ^{lm}	0.82 ± 0.002 ^{lm}	0.56 ± 0.0006 ^{cde}	0.73 ± 0.0005 ^{cd}	1.17 ± 0.001 ^f	1.46 ± 0.002 ^f	2.25 ± 0.008 ^f
100 mg L ⁻¹ Fe ₃ O ₄ NPs + 150 mg L ⁻¹ Cd	1.14 ± 0.002 ^{de}	1.09 ± 0.002 ^{fg}	0.51 ± 0.0006 ^f	0.58 ± 0.0005 ^g	0.45 ± 0.001 ^l	0.60 ± 0.002 ^k	0.76 ± 0.008 ^{kl}
100 mg L ⁻¹ n-HAP + Fe ₃ O ₄ NPs + 150 mg L ⁻¹ Cd	0.54 ± 0.002 ^p	0.41 ± 0.005 ^p	0.66 ± 0.0006 ^a	0.83 ± 0.0005 ^a	2.21 ± 0.001 ^a	2.88 ± 0.002 ^a	4.34 ± 0.008 ^a
100 mg L ⁻¹ n-HAP + 150 mg L ⁻¹ Cd	0.83 ± 0.002 ^k	0.87 ± 0.005 ^{kl}	0.55 ± 0.0006 ^{cdef}	0.69 ± 0.0005 ^{de}	1.08 ± 0.001 ^g	1.32 ± 0.002 ^g	2.01 ± 0.008 ^g
100 mg L ⁻¹ Fe ₃ O ₄ NPs + 150 mg L ⁻¹ Cd	0.76 ± 0.002 ^{lm}	0.77 ± 0.002 ^{mn}	0.56 ± 0.0006 ^{vde}	0.73 ± 0.0005 ^{cd}	1.44 ± 0.001 ^e	1.55 ± 0.002 ^e	2.67 ± 0.008 ^e
100 mg L ⁻¹ n-HAP + Fe ₃ O ₄ NPs + 150 mg L ⁻¹ Cd	1.04 ± 0.002 ^{fg}	1.01 ± 0.002 ^{hi}	0.52 ± 0.0006 ^{ef}	0.58 ± 0.0005 ^{bc}	0.61 ± 0.001 ^j	0.72 ± 0.002 ^{ij}	1.06 ± 0.008 ^j

4. Discussion

Cd (Cd), a highly toxic metal, can induce detrimental effects on animals, humans, and plants, even at low concentrations. Due to its long half-life, Cd persists in plants, interfering with their biochemical and physiological processes [59]. However, NPs (NPs), with their small size (<100 nm) and large surface area, exhibit superior reactivity compared

to larger particles, making them effective at absorbing and immobilizing metals in the soil [60]. Nano-hydroxyapatite (n-HAP) and Fe_3O_4 NPs are micronutrients that promote plant growth by enhancing root length, thus improving nutrient absorption from the soil [29]. One of the primary processes by which NPs mitigate heavy metal stress is by the exchange and absorption of metal ions on the surfaces of plant roots and leaves, hence strengthening metal tolerance [61]. Moreover, metal-based NPs can transfer metal ions into plant cells, reducing the accumulation of metals in plant organs [62]. In our previous study, we demonstrated that silicon NPs could reduce Cd accumulation in plant leaves through metal ion adsorption [63]. The foliar application of nano-hydroxyapatite (n-HAP) and iron oxide nanoparticles (Fe_3O_4 NPs) significantly reduced cadmium (Cd) bioaccumulation in bamboo plants, as demonstrated by decreased Cd concentrations in the roots, stems, and leaves. This reduction can be attributed to the dual mechanisms of Cd immobilization and adsorption facilitated by n-HAP and Fe_3O_4 NPs. Specifically, n-HAP effectively immobilized Cd in the soil and on the leaf surface through ion exchange and the formation of stable Cd–phosphate complexes [29]. Concurrently, Fe_3O_4 NPs adsorbed Cd ions and enhanced the plant's antioxidant defense system, mitigating oxidative stress induced by Cd toxicity [64]. Furthermore, the synergistic effects of these nanoparticles limited Cd translocation within the plant, thereby reducing its accumulation in above-ground organs. These findings underscore the potential of n-HAP and Fe_3O_4 NPs as effective and sustainable strategies for mitigating Cd toxicity in plants, offering promising applications in phytoremediation and agricultural practices. This reduction can be attributed to the absorption of metal ions by NPs and the redistribution of Cd in the plant tissues. Similar results have been reported for *Coriandrum sativum* L. [65] in studies using titanium dioxide NPs and for n-HAP and Fe_3O_4 on *Oryza sativa* seedlings [29]. Interestingly, in our study, the reduction in Cd in bamboo roots was more pronounced than in shoots or stems, suggesting that the combination of the two NPs was particularly effective in Cd absorption by the roots, which limited translocation to the aerial parts (Figure 8). This enhanced tolerance might show the ability of NPs to penetrate plant cells via leaf stomata and then move to the rhizome and root surface, thereby limiting Cd uptake. Similar mechanisms have been observed in cucumbers treated with different nanomaterials [66].

The unique properties of NPs, such as their high surface area, facilitate metal ion absorption through physical adsorption, likely involving Van der Waals forces, which can limit Cd uptake and reduce its transfer to plant aerial organs [67]. On the other hand, heavy metals generate ROS, leading to oxidative stress in plants [68,69]. Damaging plant membranes, proteins, and DNA disrupts water balance and ultimately hinders plant growth [70]. The application of nano-hydroxyapatite (n-HAP) and iron oxide nanoparticles (Fe_3O_4 NPs) effectively reduced cadmium (Cd) bioavailability through adsorption and immobilization mechanisms (Table 3). Additionally, their inherent antioxidant properties directly scavenged reactive oxygen species (ROS) and enhanced the activity of key antioxidant enzymes, such as superoxide dismutase (SOD) and catalase (CAT) [29]. This dual action resulted in a significant reduction in lipid peroxidation and electrolyte leakage, thereby preserving membrane integrity and alleviating oxidative stress in plants [71,72]. These findings, consistent with the results of the current study, underscore the potential of n-HAP and Fe_3O_4 NPs as protective agents against Cd-induced toxicity in plants, offering promising applications in sustainable agriculture and environmental remediation (Figure 4). Plants employ various defense strategies to scavenge ROS, with the activation of antioxidant mechanisms being a crucial response to metal stress [73]. Antioxidants like SOD, CAT, and POD convert harmful H_2O_2 into less toxic molecules, mitigating the negative effects of ROS [71]. The enhancement of antioxidant and glyoxal activity with the addition of n-HAP and Fe_3O_4 has been reported by our study (Figure 2). These increases in antioxidant

activity helped reduce ROS (H_2O_2 , $\text{O}_2^{\bullet-}$) and mitigate membrane damage by lowering MDA and EL. Additionally, NPs can enhance nutrient ion availability, which may provide essential co-factors for antioxidant synthesis, further boosting the plant's defense against oxidative stress. Similar improvements in antioxidant activity have been reported in rice seedlings exposed to Pb and Cd [29] and in pepper under Cd stress [74].

Phenolic substances, including flavonoids and phenolic acids, possess potent antioxidant capabilities attributed to their hydroxyl groups and aromatic rings, enabling effective ROS scavenging [64]. In our study, 100 mgL^{-1} n-HAP and Fe_3O_4 significantly increased total TFC and TPC in bamboo plants under Cd stress (Figure 3), helping to alleviate oxidative damage by scavenging ROS, as also observed in other studies [75,76]. This enhancement can be attributed to the ability of nano-hydroxyapatite (n-HAP) and iron oxide nanoparticles (Fe_3O_4 NPs) to reduce cadmium (Cd) uptake and bioavailability, stimulate the phenylpropanoid pathway, and supply essential nutrients such as calcium, phosphate, and iron [29]. The increased production of flavonoids and phenolics facilitated by these nanoparticles played a critical role in alleviating oxidative damage. These compounds effectively scavenged reactive oxygen species (ROS), chelated Cd ions, and protected cellular structures from oxidative stress [29]. These findings highlight the multifaceted mechanisms through which n-HAP and Fe_3O_4 NPs mitigate Cd toxicity, offering potential applications in sustainable agriculture and environmental remediation. Proline is an important osmolyte that helps plants cope with stress by stabilizing membranes, scavenging ROS, and mitigating osmotic stress [77,78]. The increasing proline accumulation in our study due to the addition of n-HAP and Fe_3O_4 NPs in bamboo plants exposed to various levels of Cd likely occurred through the regulation of gene expression related to proline biosynthesis, as demonstrated in studies on ZnO-NPs under Cd and Cu stress [79–81]. RWC is another indicator of plant water status under stress [82]. This indicator increased in this study (Figure 5), which is consistent with findings in other plants treated with NPs, such as Se-NPs on *Coriandrum sativum* under Cd stress [83]. The addition of NPs also helped regulate Fe content in bamboo leaves, preserving leaf structure and maintaining RWC, which is crucial for plant development [84]. Moreover, nitric oxide (NO) is essential for increasing water content by facilitating cell wall extensibility, assisting cell division, and promoting leaf area growth [85]. In this study, the increased NO content occurred with the addition of NPs in Cd-stressed bamboo plants (Figure 5). This increase in NO was linked to improved RWC, as previously observed in our work [86]. The observed increase in nitric oxide (NO) levels can be attributed to the ability of nano-hydroxyapatite (n-HAP) and iron oxide nanoparticles (Fe_3O_4 NPs) to reduce cadmium (Cd) uptake and toxicity, stimulate NO biosynthesis, and effectively scavenge reactive oxygen species (ROS). NO, in turn, played a protective role by regulating stomatal closure, promoting the accumulation of osmoprotectants, and preserving membrane integrity, all of which contributed to improved relative water content (RWC) [87]. These findings highlight the multifaceted mechanisms through which n-HAP and Fe_3O_4 NPs mitigate Cd-induced stress, offering potential applications in sustainable agriculture and environmental remediation. Finally, heavy metal stress can damage plant photosynthesis by generating ROS that disrupt chloroplast function, leading to reduced growth [64]. However, the application of NPs helped preserve chlorophyll integrity and improved photosynthetic efficiency by protecting chloroplast enzymes and reducing free radical accumulation [88]. The results showed that n-HAP and Fe_3O_4 NPs promoted gas exchange and chlorophyll in bamboo species under Cd stress. This enhancement of photosynthetic efficiency is consistent with studies showing that NPs increase antioxidant capacity and improve growth [89]. Thus, the application of n-HAP and Fe_3O_4 NPs, both individually and in combination, promoted bamboo growth and development under Cd stress. This was achieved through enhanced antioxidant activity, reduced Cd

bioaccumulation, improved water content, and optimized photosynthetic efficiency. These findings underscore the potential of n-HAP and Fe₃O₄ NPs as a tool for mitigating heavy metal toxicity and promoting plant tolerance under stress conditions.

5. Conclusions

This study was conducted in a greenhouse to examine the potential of foliar applications of n-HAP and Fe₃O₄ NPs to enhance bamboo tolerance to Cd toxicity. Exposure to Cd concentrations (50, 80, 100, and 150 mgL⁻¹) impaired plant growth by inducing oxidative stress, limiting water availability, and reducing photosynthesis and biomass. Foliar treatments of 100 mgL⁻¹ n-HAP and 100 mgL⁻¹ Fe₃O₄ NPs, individually/in combination, significantly improved plant growth under Cd stress through enhanced antioxidants (SOD, CAT, PAL, POD, GR) and glyoxalase activities (GLyI, GLyII) and increased levels of TFC and TPC (non-antioxidants). Additionally, the treatments improved RWC, proline accumulation, and nitric oxide levels. NPs also reduced membrane leakage, scavenged ROS (H₂O₂ and O₂^{•-}), and enhanced cell protection. Furthermore, NPs optimized gas exchange, maintained chlorophyll integrity, and increased photosynthetic rate, contributing to greater plant biomass. These data suggest that n-HAP and Fe₃O₄ NPs mitigate Cd toxicity by limiting Cd uptake and translocation, enhancing antioxidants and non-antioxidants, and improving plant water status. Although both single and combined NPs alleviated Cd toxicity, the combination of 100 mgL⁻¹ n-HAP and Fe₃O₄ NPs demonstrated the most significant impact on bamboo tolerance. However, further research is required to explore additional mechanisms involved in this process. However, the findings are constrained by several limitations, including controlled experimental conditions, short-term evaluation, and a lack of detailed mechanistic insights into the molecular pathways involved. To address these limitations, future research should prioritize field trials, dose–response studies, and long-term monitoring to validate the efficacy and sustainability of nano-hydroxyapatite (n-HAP) and iron oxide nanoparticles (Fe₃O₄ NPs) in mitigating heavy metal stress. Furthermore, investigating the molecular mechanisms, synergistic effects with other soil amendments, and potential environmental risks associated with nanoparticle application will provide a more comprehensive understanding of their practical use. These efforts are essential to advance the safe and effective implementation of nanotechnology in agriculture and environmental remediation, particularly in enhancing plant resilience to combined abiotic stresses.

Author Contributions: Conceptualization, A.E., A.K. and N.P.; methodology, A.E. and Y.L.; software, Y.L.; validation, A.E., A.K. and N.P.; formal analysis, Y.L.; investigation, A.E.; resources, A.E.; data curation, A.E.; writing—original draft preparation, A.E., A.K., N.P. and Y.L.; writing—review and editing, A.E., A.K., N.P. and Y.L.; visualization, A.E.; supervision, A.E.; project administration, A.E.; funding acquisition, A.K. All authors have read and agreed to the published version of the manuscript.

Funding: The authors extend their appreciation to the Deanship of Research and Graduate Studies at King Khalid University for funding this work through a large Research Project under grant number RGP2/526/45.

Data Availability Statement: The data presented in this study are available in the article.

Conflicts of Interest: The authors declare no conflicts of interest.

References

1. Bhat, J.A.; Shivaraj, S.M.; Singh, P.; Navadagi, D.B.; Tripathi, D.K.; Dash, P.K.; Solanke, A.U.; Sonah, H.; Deshmukh, R. Role of silicon in mitigation of heavy metal stresses in crop plants. *Plants* **2019**, *21*, 71. [[CrossRef](#)]
2. Emamverdian, A.; Ding, Y. Effects of heavy metals' toxicity on plants and enhancement of plant defense mechanisms of Si-mediation. *Int. J. Environ. Agric. Res.* **2017**, *3*, 41–51.

3. Kim, J.J.; Kim, Y.S.; Kumar, V. Heavy metal toxicity: An update of chelating therapeutic strategies. *J. Trace Elem. Med. Biol.* **2019**, *54*, 226–231. [[CrossRef](#)]
4. Qi, Z.Y.; Ahammed, G.J.; Jiang, C.Y.; Li, C.X.; Zhou, J. E3 ubiquitin ligase gene SIRING1 is essential for plant tolerance to Cd stress in *Solanum lycopersicum*. *J. Biotechnol.* **2020**, *20*, 239–247. [[CrossRef](#)] [[PubMed](#)]
5. Ghorbani, A.; Emamverdian, A.; Pehlivan, N.; Zargar, M.; Razavi, S.M.; Chen, M. Nano-enabled agrochemicals: Mitigating heavy metal toxicity and enhancing crop adaptability for sustainable crop production. *J. Nanobiotechnol.* **2024**, *22*, 91. [[CrossRef](#)] [[PubMed](#)]
6. Chen, R.; De Sherbinin, A.; Ye, C.; Shi, G. China's soil pollution: Farms on the frontline. *Science* **2014**, *344*, 691. [[CrossRef](#)] [[PubMed](#)]
7. Zhang, X.; Zhong, T.; Liu, L.; Ouyang, X. Impact of soil heavy metal pollution on food safety in China. *PLoS ONE* **2015**, *10*, e0135182. [[CrossRef](#)]
8. Rian, Y.; He, L.; Cai, R.; Li, B.; Li, Z.; Yang, K. Heavy metal pollution and health risk in China. *Glob. Health J.* **2017**, *1*, 47–55.
9. Qin, Q.; Li, X.; Wu, H.; Zhang, Y.; Feng, Q.; Tai, P. Characterization of cadmium (108Cd) distribution and accumulation in *Tagetes erecta* L. seedlings: Effect of split-root and of remove-xylem/phloem. *Chemosphere* **2013**, *93*, 2284–2288. [[CrossRef](#)]
10. Adrees, M.; Ali, S.; Rizwan, M.; Zia-ur-Rehman, M.; Ibrahim, M.; Abbas, F.; Farid, M.; Qayyum, M.F.; Irshad, M.K. Mechanisms of silicon-mediated alleviation of heavy metal toxicity in plants: A review. *Ecotoxicol. Environ. Saf.* **2015**, *119*, 186–197. [[CrossRef](#)] [[PubMed](#)]
11. Emamverdian, A.; Ding, Y.; Barker, J.; Liu, G.; Hasanuzzaman, M.; Li, Y.; Ramakrishnan, M.; Mokhberdorran, F. Co-Application of 24-Epibrassinolide and Titanium Oxide NPs Promotes *Pleioblastus pygmaeus* Plant Tolerance to Cu and Cd Toxicity by Increasing Antioxidant Activity and Photosynthetic Capacity and Reducing Heavy Metal Accumulation and Translocation. *Antioxidants* **2022**, *11*, 451. [[CrossRef](#)] [[PubMed](#)]
12. Singh, S.; Susan, E.; D'Souza, S.F. Cd accumulation and its influence on lipid peroxidation and antioxidative system in an aquatic plant, *Bacopa monnieri* L. *Chemosphere* **2006**, *62*, 233–246. [[CrossRef](#)] [[PubMed](#)]
13. Tortella, G.R.O.; Rubilar, N.; Duran, M.C.; Diez, M.; Martinez, J.; Parada, A.B. Seabra Silver NPs: Toxicity in model organisms as an overview of its hazard for human health and the environment. *J. Hazard. Mater.* **2020**, *390*, 121974. [[CrossRef](#)] [[PubMed](#)]
14. Singh, R.; Bhatia, R. Experimental and modeling process optimization of lead adsorption on magnetite NPs via isothermal, kinetics, and thermodynamic studies. *ACS Omega* **2020**, *5*, 10826–10837. [[CrossRef](#)] [[PubMed](#)]
15. Tang, J.; Su, M.; Wu, Q.; Wei, L.; Wang, N.; Xiao, E.; Zhang, H.; Wei, Y.; Liu, Y.; Ekberg, C.; et al. Highly efficient recovery and clean-up of four heavy metals from MSWI fly ash by integrating leaching, selective extraction and adsorption. *J. Clean. Prod.* **2019**, *234*, 139–149. [[CrossRef](#)]
16. Li, J.; Hu, J.; Xiao, L.; Wang, Y.; Wang, X. Interaction mechanisms between α -Fe₂O₃, γ -Fe₂O₃ and Fe₃O₄ NPs and *Citrus maxima* seedlings. *Sci. Total Environ* **2018**, *625*, 677–685. [[CrossRef](#)]
17. Yuan, J.; Chen, Y.; Li, H.; Lu, J.; Zhao, H.; Liu, M.; Nechitaylo, G.S.; Glushchenko, N.N. New insights into the cellular responses to iron NPs in *Capsicum annum*. *Sci. Rep.* **2018**, *8*, 3228. [[CrossRef](#)] [[PubMed](#)]
18. Gupta, N.; Singh, P.M.; Sagar, V.; Pandya, A.; Chinnappa, M.; Kumar, R.; Bahadur, A. Seed priming with ZnO and Fe₃O₄ NPs alleviate the lead toxicity in *Basella alba* L. Through reduced lead uptake and regulation of ROS. *Plants* **2022**, *11*, 2227. [[CrossRef](#)] [[PubMed](#)]
19. Konate, A.; He, X.; Zhang, Z.; Ma, Y.; Zhang, P.; Alugongo, G.; Rui, Y. Magnetic (Fe₃O₄) NPs reduce heavy metals uptake and mitigate their toxicity in wheat seedling. *Sustainability* **2017**, *9*, 790. [[CrossRef](#)]
20. Shaheen, S.M.; Rinklebe, J. Impact of emerging and low cost alternative amendments on the (im)mobilization and phytoavailability of Cd and Pb in a contaminated floodplain soil. *Ecol. Eng* **2015**, *74*, 319–326. [[CrossRef](#)]
21. Yan, Y.; Qi, F.; Zhao, S.; Luo, Y.; Gu, S.; Li, Q.; Zhang, L.; Zhou, S.; Bolan, N. A new low-cost hydroxyapatite for efficient immobilization of lead. *J. Colloid Interface Sci.* **2019**, *553*, 798–804. [[CrossRef](#)] [[PubMed](#)]
22. Feng, Y.; Yang, J.; Liu, W.; Yan, Y.; Wang, Y. Hydroxyapatite as a passivator for safe wheat production and its impacts on soil microbial communities in a Cd-contaminated alkaline soil. *J. Hazard. Mater.* **2021**, *404 Pt B*, 124005. [[CrossRef](#)]
23. Liu, R.; Lal, R. Synthetic apatite nanoparticles as a phosphorus fertilizer for soybean (*Glycine max*). *Sci Rep.* **2014**, *4*, 5686. [[CrossRef](#)]
24. Kottegoda, N.; Sandaruwan, C.; Priyadarshana, G.; Siriwardhana, A.; Rathnayake, U.A.; Berugoda Arachchige, D.M.; Kumarasinghe, A.R.; Dahanayake, D.; Karunaratne, V.; Amaratunga, G.A. Urea-Hydroxyapatite Nanohybrids for Slow Release of Nitrogen. *ACS Nano* **2017**, *11*, 1214–1221. [[CrossRef](#)] [[PubMed](#)]
25. Silva, M.M.; Pérez, D.V.; Wasserman, J.C.; Santos-Oliveira, R.; Wasserman, M.A.V. The effect of nanohydroxyapatite on the behavior of metals in a microcosm simulating a lentic environment. *Environ. Nanotechnol. Monit. Manag.* **2017**, *8*, 219–227.
26. Huang, R.; Mao, P.; Xiong, L.; Qin, G.; Zhou, J.; Zhang, J.; Li, Z.; Wu, J. Negatively charged nano-hydroxyapatite can be used as a phosphorus fertilizer to increase the efficacy of wollastonite for soil cadmium immobilization. *J. Hazard. Mater.* **2023**, *443 Pt B*, 130291. [[CrossRef](#)]

27. Zhao, C.; Ren, S.; Zuo, Q.; Wang, S.; Zhou, Y.; Liu, W.; Liang, S. Effect of nanohydroxyapatite on cadmium leaching and environmental risks under simulated acid rain. *Sci. Total Environ.* **2018**, *627*, 553–560. [[CrossRef](#)] [[PubMed](#)]
28. Khan, S.; Akhtar, N.; Rehman, S.U.; Shujah, S.; Rha, E.S.; Jamil, M. *Bacillus subtilis* Synthesized Iron Oxide Nanoparticles (Fe₃O₄ NPs) Induced Metabolic and Anti-Oxidative Response in Rice (*Oryza sativa* L.) under Arsenic Stress. *Toxics* **2022**, *10*, 618. [[CrossRef](#)]
29. Wu, H.; Jiang, X.; Tong, J.; Wang, J.; Shi, J. Effects of Fe₃O₄ NPs and nano hydroxyapatite on Pb and Cd stressed rice (*Oryza sativa* L.) seedling. *Chemosphere* **2023**, *329*, 138686. [[CrossRef](#)] [[PubMed](#)]
30. Liang, S.X.; Jin, Y.; Liu, W.; Li, X.; Shen, S.G.; Ding, L. Feasibility of Pb phytoextraction using nano-materials assisted ryegrass: Results of a one-year field-scale experiment. *J. Environ. Manag.* **2017**, *190*, 170–175. [[CrossRef](#)]
31. Kumar, V.; Guleria, P.; Ranjan, S. Phytoresponse to nanoparticle exposure. *Nanotoxicol. Nanoecotoxicol.* **2021**, *1*, 251–286.
32. Ahmad, Z.; Upadhyay, A.; Ding, Y.; Emamverdian, A.; Shahzad, A. Bamboo: Origin, habitat, distributions and global prospective. In *Biotechnological Advances in Bamboo*; Ahmad, Z., Ding, Y., Shahzad, A., Eds.; Springer: Singapore, 2021.
33. Emamverdian, A.; Ding, Y.; Mokhberdoran, F.; Xie, Y. Growth responses and photosynthetic indices of Bamboo plant (*Indocalamus latifolius*) under heavy metal stress. *Sci. World J.* **2018**, *2018*, 1219364. [[CrossRef](#)]
34. Emamverdian, A.; Ding, Y.; Mokhberdoran, F.; Ramakrishnan, M.; Ahmad, Z.; Xie, Y. Different physiological and biochemical responses of bamboo to the addition of TiO₂ NPs under HM toxicity. *Forests* **2021**, *12*, 759. [[CrossRef](#)]
35. Bian, F.; Zhong, Z.; Zhang, X.; Yang, C.; Gai, X. Bamboo—An untapped plant resource for the phytoremediation of heavy metal contaminated soils. *Chemosphere* **2019**, *246*, 125750. [[CrossRef](#)] [[PubMed](#)]
36. Liu, J.N.; Zhou, Q.X.; Sun, T.; Ma, L.Q.; Wang, S. Growth responses of three ornamental plants to Cd and Pb stress and their metal accumulation characteristics. *J. Hazard. Mater.* **2008**, *151*, 261–267. [[CrossRef](#)]
37. González-Chávez Mdel, C.; Carrillo-González, R. Tolerance of *Chrysanthemum maximum* to heavy metals: The potential for its use in the revegetation of tailings heaps. *J. Environ. Sci.* **2013**, *25*, 367–375. [[CrossRef](#)] [[PubMed](#)]
38. Emamverdian, A.; Khalofah, A.; Pehlivan, N.; Li, Y.; Chen, M.; Liu, G. Iron NPs in combination with other conventional Fe sources remediate mercury toxicity-affected plants and soils by nutrient accumulation in bamboo species. *Ecotoxicol. Environ. Saf.* **2024**, *278*, 116431. [[CrossRef](#)] [[PubMed](#)]
39. Emamverdian, A.; Khalofah, A.; Pehlivan, N.; Zia-ur-Rehman, M.; Li, Y.; Zargar, M. Exogenous application of jasmonates and brassinosteroids alleviates lead toxicity in bamboo by altering biochemical and physiological attributes. *Environ. Sci. Pollut. Res.* **2024**, *31*, 7008–7026. [[CrossRef](#)]
40. Senthilkumar, M.; Amaresan, N.; Sankaranarayanan, A. Estimation of superoxide dismutase (SOD). In *Plant-Microbe Interactions*; Springer: Berlin/Heidelberg, Germany, 2021; pp. 117–118.
41. Berner, M.; Krug, D.; Bihlmaier, C.; Vente, A.; Müller, R.; Bechthold, A. Genes and enzymes involved in caffeic acid biosynthesis in the actinomycete *Saccharothrix espanaensis*. *J. Bacteriol.* **2006**, *188*, 2666–2673. [[CrossRef](#)] [[PubMed](#)]
42. Aebi, H. Catalase in vitro. *Methods Enzymol.* **1984**, *105*, 121–126.
43. Liu, N.; Lin, Z.; Guan, L.; Gaughan, G.; Lin, G. Antioxidant enzymes regulate reactive oxygen species during pod elongation in *Pisum sativum* and *Brassica chinensis*. *PLoS ONE* **2014**, *9*, e87588. [[CrossRef](#)] [[PubMed](#)]
44. Foyer, C.H.; Halliwell, B. The presence of glutathione and glutathione reductase in chloroplasts: A proposed role in ascorbic acid metabolism. *Planta* **1976**, *133*, 21–25. [[CrossRef](#)] [[PubMed](#)]
45. Hasanuzzaman, M.; Hossain, M.A.; Fujita, M. Nitric oxide modulates antioxidant defense and the methylglyoxal detoxification system and reduces salinity-induced damage of wheat seedlings. *Plant Biotechnol. Rep.* **2011**, *5*, 353. [[CrossRef](#)]
46. Principato, G.B.; Rosim, G.; Talesam, V.; Giovannini, E.; Uotila, L. Purification and characterization of two forms of glyoxalase II from the liver and brain of Wistar rats. *Biochim. Biophys. Acta* **1987**, *911*, 349–355. [[CrossRef](#)]
47. Yadav, S.K.; Singla-Pareek, S.L.; Reddy, M.K.; Sopory, S.K. Trans-genic tobacco plants overexpressing glyoxalase enzymes resist an increase in methylglyoxal and maintain higher reduced glutathione levels under salinity stress. *FEBS Lett.* **2005**, *579*, 6265–6271. [[CrossRef](#)]
48. McDonald, S.; Prenzler, P.D.; Antolovich, M.; Robards, K. Phenolic content and antioxidant activity of olive extracts. *Food Chem.* **2001**, *73*, 73–84. [[CrossRef](#)]
49. Chang, C.C.; Yang, M.H.; Wen, H.M.; Chern, J.C. Estimation of total flavonoid content in propolis by two complementary colorimetric methods. *J. Food Drug Anal.* **2002**, *10*, 178–182.
50. Rao, K.M.; Sresty, T. Antioxidative parameters in the seedlings of pigeonpea (*Cajanus cajan* (L.) Millspaugh) in response to Zn and Ni stresses. *Plant Sci.* **2000**, *157*, 113–128.
51. Velikova, V.; Yordanov, I.; Edreva, A. Oxidative stress and some antioxidant systems in acid rain-treated bean plants: Protective role of exogenous polyamines. *Plant Sci.* **2000**, *151*, 59–66. [[CrossRef](#)]
52. Valentovic, P.; Luxova, M.; Kolarovic, L.; Gasparikova, O. Effect of osmotic stress on compatible solutes content, membrane stability and water relations in two maize cultivars. *Plant Soil Environ.* **2006**, *52*, 186–191. [[CrossRef](#)]

53. Bates, L.S.; Walden, R.P.; Teare, I.D. Rapid determination of free proline for water stress studies. *Plant Soil* **1973**, *39*, 205–207. [[CrossRef](#)]
54. Dhopte, A.M.; Manuel, L.M. Principles and techniques for plant scientists. In *Updesh Purohit for Agrobios*, 1st ed.; Agrobios: Jodhpur, India, 2002; Volume 81, p. 373.
55. Arnon, D.I. Copper enzymes in isolated chloroplasts. Polyphenoloxidase in *Beta vulgaris*. *Plant Physiol.* **1949**, *24*, 1–15. [[CrossRef](#)]
56. Holá, D.; Benešová, M.; Honnerová, J.; Hnilická, F.; Rothová, O.; Kocová, M.; Hnilíčková, H. The evaluation of photo-synthetic parameters in maize inbred lines subjected to water deficiency: Can these parameters be used for the prediction of performance of hybrid progeny? *Photosynthetica* **2010**, *48*, 545–558. [[CrossRef](#)]
57. Khosropour, E.; Attarod, P.; Shirvany, A.; Pypker, T.G.; Bayramzadeh, V.; Hakimi, L.; Moeinaddini, M. Response of *Platanus orientalis* leaves to urban pollution by HMs. *J. For. Res.* **2019**, *30*, 1437–1445. [[CrossRef](#)]
58. Souri, Z.; Karimi, N. Enhanced Phytoextraction by as Hyperaccumulator *Isatis cappadocica* Spiked with Sodium Nitro-prusside. *Soil Sediment Contam. Int. J.* **2017**, *26*, 457–468. [[CrossRef](#)]
59. Soni, S.; Jha, A.B.; Dubey, R.S.; Sharma, P. Mitigating Cd accumulation and toxicity in plants: The promising role of NPs. *Sci. Total Environ.* **2024**, *912*, 168826. [[CrossRef](#)]
60. Liu, W.; Li, Y.; Feng, Y.; Qiao, J.; Zhao, H.; Xie, J.; Fang, Y.; Shen, S.; Liang, S. The effectiveness of nanobiochar for reducing phytotoxicity and improving soil remediation in Cd-contaminated soil. *Sci. Rep.* **2020**, *10*, 858.
61. Zhou, P.; Adeel, M.; Shakoor, N.; Guo, M.; Hao, Y.; Azeem, I.; Li, M.; Liu, M.; Rui, Y. Application of NPs Alleviates Heavy Metals Stress and Promotes Plant Growth: An Overview. *Nanomaterials* **2020**, *11*, 26. [[CrossRef](#)] [[PubMed](#)]
62. Mihailovic, V.; Katanic Stankovic, J.S.; Selakovic, D.; Rosic, G. An Overview of the Beneficial Role of Antioxidants in the Treatment of Nanoparticle-Induced Toxicities. *Oxid. Med. Cell. Longev.* **2021**, *15*, 7244677. [[CrossRef](#)]
63. Emamverdian, A.; Ding, Y.; Mokberdorran, F.; Ahmad, Z.; Xie, Y. Determination of HMs tolerance threshold in a bamboo species (*Arundinaria pygmaea*) as treated with silicon dioxide NPs. *Glob. Ecol. Conserv.* **2020**, *24*, e0130.
64. Rizwan, M.; Ali, S.; Ali, B.; Adrees, M.; Arshad, M.; Hussain, A.; ur Rehman, M.Z.; Waris, A.A. Zinc and iron oxide nanoparticles improved the plant growth and reduced the oxidative stress and cadmium concentration in wheat. *Chemosphere* **2019**, *214*, 269–277. [[CrossRef](#)] [[PubMed](#)]
65. Sardar, R.; Ahmed, S.; Yasin, N.A. Titanium dioxide NPs mitigate Cd toxicity in *Coriandrum sativum* L. through modulating antioxidant system, stress markers and reducing Cd uptake. *Environ. Pollut.* **2022**, *292 Pt A*, 118373. [[CrossRef](#)]
66. Guo, K.; Hu, A.; Wang, K.; Wang, L.; Fu, D.; Hao, Y.; Wang, Y.; Ali, A.; Adeel, M.; Rui, Y.; et al. Effects of spraying nanomaterials on the absorption of metal(loid)s in cucumber. *IET Nanobiotechnol.* **2019**, *13*, 712–719. [[CrossRef](#)] [[PubMed](#)]
67. Burakov, A.E.; Galunin, E.V.; Burakova, I.V.; Kucherova, A.E.; Agarwal, S.; Tkachev, A.G.; Gupta, V.K. Adsorption of heavy metals on conventional and nanostructured materials for wastewater treatment purposes: A review. *Ecotoxicol. Environ. Saf.* **2018**, *148*, 702–712. [[CrossRef](#)]
68. Wani, K.I.; Naeem, M.; Castroverde, C.D.M.; Kalaji, H.M.; Albaqami, M.; Aftab, T. Molecular mechanisms of nitric oxide (NO) signaling and reactive oxygen species (ROS) homeostasis during abiotic stresses in plants. *Int. J. Mol. Sci.* **2021**, *22*, 9656. [[CrossRef](#)] [[PubMed](#)]
69. Gechev, T.; Petrov, V. Reactive oxygen species and abiotic stress in plants. *Int. J. Mol. Sci.* **2020**, *21*, 7433. [[CrossRef](#)] [[PubMed](#)]
70. Akhtar, N.; Khan, S.; Rehman, S.U.; Rehman, Z.U.; Khatoon, A.; Rha, E.S.; Jamil, M. Synergistic Effects of Zinc Oxide Nanoparticles and Bacteria Reduce Heavy Metals Toxicity in Rice (*Oryza sativa* L.). *Plant. Toxicol.* **2021**, *9*, 113. [[CrossRef](#)]
71. Emamverdian, A.; Ghorbani, A.; Pehlivan, N.; Li, Y.; Zargar, M.; Liu, G. Bamboo biochar helps minimize *Brassica* phytotoxicity driven by toxic metals in naturally polluted soils of four mine zones. *Environ. Technol. Innov.* **2024**, *36*, 103753. [[CrossRef](#)]
72. Emamverdian, A.; Ghorbani, A.; Pehlivan, N.; Barker, J.; Zargar, M.; Chen, M.; Liu, G. Brassinolide ameliorates the detrimental effects of arsenic in tomato: Insights into iron and arsenic absorption, antioxidant capacity, nitrogen, and sulfur assimilation. *Hortic. Plant J.* **2024**, *in press*. [[CrossRef](#)]
73. Jiang, D.; Hou, J.; Gao, W.; Tong, X.; Li, M.; Chu, X. Exogenous spermidine alleviates the adverse effects of aluminum toxicity on photosystem II through improved antioxidant system and endogenous polyamine contents. *Ecotoxicol. Environ. Saf.* **2021**, *207*, 111265. [[CrossRef](#)]
74. Mozafariyan, M.; Shekari, L.; Hawrylak-Nowak, B.; Kamelmanesh, M.M. Protective Role of Selenium on Pepper Exposed to Cd Stress During Reproductive Stage. *Biol. Trace Elem. Res.* **2014**, *160*, 97–107. [[CrossRef](#)]
75. Babashpour-Asl, M.; Farajzadeh-Memari-Tabrizi, E.; Yousefpour-Dokhanieh, A. Foliar-applied selenium NPs alleviate Cd stress through changes in physio-biochemical status and essential oil profile of coriander (*Coriandrum sativum* L.) leaves. *Environ. Sci. Pollut. Res.* **2022**, *29*, 80021–80031. [[CrossRef](#)] [[PubMed](#)]
76. Memari-Tabrizi, E.F.; Yousefpour-Dokhanieh, A.; Babashpour-Asl, M. Foliar-applied silicon NPs mitigate Cd stress through physio-chemical changes to improve growth, antioxidant capacity, and essential oil profile of summer savory (*Satureja hortensis* L.). *Plant Physiol. Biochem.* **2021**, *165*, 71–79. [[CrossRef](#)] [[PubMed](#)]

77. Bandurska, H. Does proline accumulated in leaves of water deficit stressed barley plants confine cell membrane injuries? II. Proline accumulation during hardening and its involvement in reducing membrane injuries in leaves subjected to severe osmotic stress. *Acta Physiol. Plant.* **2001**, *23*, 483–490. [[CrossRef](#)]
78. Torabian, S.; Zahedi, M.; Khoshgoftarmanesh, A. Effect of foliar spray of zinc oxide on some antioxidant enzymes activity of sunflower under salt stress. *J. Agric. Sci. Technol.* **2016**, *18*, 1013–1025. Available online: <http://jast.modares.ac.ir/article-23-5061-en.html> (accessed on 1 January 2020).
79. Faizan, M.; Bhat, J.A.; Noureldeen, A.; Ahmad, P.; Yu, F. Zinc oxide NPs and 24-epibrassinolide alleviates Cu toxicity in tomato by regulating ROS scavenging, stomatal movement and photosynthesis. *Ecotoxicol. Environ. Saf.* **2021**, *218*, 112293. [[CrossRef](#)] [[PubMed](#)]
80. Helaly, M.N.; El-Metwally, M.A.; El-Hoseiny, H.; Omar, S.A.; El-Sheery, N.I. Effect of NPs on biological contamination of in vitro cultures and organogenic regeneration of banana. *Aust. J. Crop. Sci.* **2014**, *8*, 612–624.
81. Emamverdian, A.; Ding, Y.; Mokhberdoran, F.; Ahmad, Z.; Xie, Y. The Investigation of TiO₂ NPs Effect as a Wastewater Treatment to Mitigate Cd Negative Impact on Bamboo Growth. *Sustainability* **2021**, *13*, 3200. [[CrossRef](#)]
82. Ahmed, T.; Noman, M.; Ijaz, M.; Ali, S.; Rizwan, M.; Ijaz, U.; Hameed, A.; Ahmad, U.; Wang, Y.; Sun, G.; et al. Current trends and future prospective in nanoremediation of HMs contaminated soils: A way forward towards sustainable agriculture. *Ecotoxicol. Environ. Saf.* **2021**, *227*, 112888. [[CrossRef](#)] [[PubMed](#)]
83. Sardar, R.; Ahmed, S.; Sha, A.A.; Yasin, N.A. Selenium NPs reduced Cd uptake, regulated nutritional homeostasis and antioxidant system in *Coriandrum sativum* grown in Cd toxic conditions. *Chemosphere* **2022**, *287*, 132332. [[CrossRef](#)]
84. Shirani Bidabadi, S.; Sabbatini, P.; Vander Weide, J. Iron oxide (IO) NPs alleviate PEG-simulated drought stress in grape (*Vitis vinifera* L.) plants by regulating leaf antioxidants. *Sci. Hortic.* **2023**, *312*, 111847. [[CrossRef](#)]
85. Ahmad, P.; Ahanger, M.A.; Alyemeni, M.N.; Wijaya, L.; Alam, P. Exogenous application of nitric oxide modulates osmolyte metabolism, antioxidants, enzymes of ascorbate-glutathione cycle and promotes growth under Cd stress in tomato. *Protoplasma* **2018**, *255*, 79–93. [[CrossRef](#)] [[PubMed](#)]
86. Emamverdian, A.; Ding, Y.; Barker, J.; Liu, G.; Li, Y.; Mokhberdoran, F. Sodium Nitroprusside Improves Bamboo Resistance under Mn and Cr Toxicity with Stimulation of Antioxidants Activity, Relative Water Content, and Metal Trans-location and Accumulation. *Int. J. Mol. Sci.* **2023**, *24*, 1942. [[CrossRef](#)]
87. Nabi, R.B.S.; Tayade, R.; Hussain, A.; Kulkarni, K.P.; Imran, Q.M.; Mun, B.G.; Yun, B.W. Nitric oxide regulates plant responses to drought, salinity, and heavy metal stress. *Environ. Exp. Bot.* **2019**, *161*, 120–133. [[CrossRef](#)]
88. El-Badri, A.M.; Hashem, A.M.; Batool, M.; Sherif, A.; Nishawy, E.; Ayaad, M.; Hassan, H.M.; Elrewainy, I.M.; Wang, J.; Kuai, J.; et al. Comparative efficacy of bio-selenium NPs and sodium selenite on mor-pho-physiochemical attributes under normal and salt stress conditions, besides selenium detoxification pathways in *Brassica napus* L. *J. Nanobiotechnol.* **2022**, *20*, 163. [[CrossRef](#)] [[PubMed](#)]
89. Moussa, H.R.; El-Fatah, A.; Ahmed, M. Protective role of selenium on development and physiological responses of *Vicia faba*. *Int. J. Veg. Sci.* **2010**, *16*, 174–183. [[CrossRef](#)]

Disclaimer/Publisher’s Note: The statements, opinions and data contained in all publications are solely those of the individual author(s) and contributor(s) and not of MDPI and/or the editor(s). MDPI and/or the editor(s) disclaim responsibility for any injury to people or property resulting from any ideas, methods, instructions or products referred to in the content.